Comparison of Equilibrium-Stage and Rate Based Model of an Absorption Column for a CO2-MEA system

Pranav Balvalli

Master Thesis

TU Delft Delft University of Technology

Comparison of Equilibrium-Stage and Rate Based Model of an Absorption Column for a CO2-MEA system

By

Pranav Balvalli

in partial fulfilment of the requirements for the degree of
Master of Science
in Mechanical Engineering
at the Delft University of Technology

Supervisor:	Prof. Dr. Ir. T.J. H. Vlugt
	Dr. Ir. Marco W.M. van Goethem
Committee :	Prof. Dr. Ir. T.J. H. Vlugt
	Dr. Ir. Marco W.M. van Goethem
	Dr. Ir. H.J.M. Kramer
	Dr. Ir. M.Ramdin
	Prof. Dr. W. Buijs

Faculty of Mechanical, Maritime and Materials Engineering (3mE) · Delft University of Technology


TU Delft
Delft
University of
Technology


Technip

Table of Contents

List of Figures

List of Tables

Preface

This thesis is the result of my Master of Science research project at TU Delft. This project has been carried out at Technip Benelux B.V. in collaboration with TU Delft.

Abstract

The desorption step of the carbon dioxide absorption/desorption process is an extremely energy intensive process, which accounts for 70% of operating cost according to Mofarahi et al. [2008]. Technip-ECN has proposed a solution of Heat integrated absorption column. In order to develop a model for this new column, an equation based model of the regular absorption column was required to be made where the equations are written in residual form so that the programmer has control over the parameters and equations. In this study, two models of carbon dioxide absorption were developed in Python^{TM} which represent the two different approaches that exist in literature, namely the rate based model and the equilibrium model. These models are then compared against each other on the basis of their ability to predict experimental data in four varying conditions. The key research question is to find out if the models can predict the temperature bulge inside the absorption column and what factors affect the position and shape of the temperature bulge. The results show that the rate based model gives better predictions as compared to the equilibrium model. The rate based model further reveals that competing absorption and evaporation processes produce the temperature bulge and that the position and shape of the bulge can be changed by changing the extent of absorption and evaporation. It is observed that the results of the rate based model are dependent on the model parameters such as correlations for mass transfer coefficient, enhancement factors, rate constants etc. This model is recommended to be used in the second stage of the project.

Acknowledgments

I would like to express my gratitude to Marco van Goethem who gave me the great opportunity to do this interesting project at Technip as well as his continuous support and help with this project. I would also like to thank, Prof. Thijs Vlugt his guidance throughout the project.

Finally, I want to thank my parents for their support and motivation throughout my masters program.

List of Symbols

ρ	[kg/m^3]	Density
g	[m/s^2]	Acceleration due to gravity
P	[Pa]	Pressure
Re	[-]	Reynolds number
μ	[Pas]	Dynamic viscosity
Q	[kW]	Heat Added
C_p	[J/kgK]	Specific heat capacity
ξ	[-]	Extent of Reaction
N	[mol/s]	Number of moles
ν	[-]	Stoichiometric number
a	[-]	Activity
$M_{w,L}$	[kg/kmole]	Average molar mass of amine solution
λ	[W/(mK)]	Thermal conductivity
γ	[-]	Activity coefficient
y	[-]	Gas mole fraction
x	[-]	Liquid Mole fraction
K	[mol/dm^3]	Equilibrium constant
H	[kW]	Enthalpy
C_l	[-]	Constant for liquid mass transfer coefficient of Billet and Schultes [1999]
C_g	[-]	Constant for gas mass transfer coefficient of Billet and Schultes [1999]
$He_{x,y}$	[Pam^{3}mol^{-1}]	Henry's Constant of x in y
k_2	[m^{3}mol^{-1}s^{-1}]	Rate Constant
E	[-]	Enhancement Factor
E_∞	[-]	Enhancement factor (instaneous reaction)
$D_{i,L}$	[m^{2}s^{-1}]	Diffusivity of i in liquid
E_1	[-]	Factor for calculating Enhancement factor Wellek et al. [1978]
M	[-]	Dimensionless number used in Enhancement factor

n	[-]	Factor used for Enhancement factor of van Krevelen and Hoftijzer [1948]
k_L	[m/s]	Mass transfer coefficient of liquid
k_G	[m/s]	Mass transfer coefficient of gas
K_{CO_2}	[Pa]	Henry's constant and chemical equilibrium combined by Gabrielsen et al. [2006]
Re_L	[-]	Reynolds number
a_w	[m^2m^{-3}]	Specific wetted area for mass transfer
A_C	[m^2]	Cross sectional area of the column
μ_L	[Pas]	Liquid viscosity
d_h	[m]	Hydraulic diameter
ϵ	[m^3m^{-3}]	Void fraction
ν	[m^2s^{-1}]	Kinematic viscosity
h	[$Jmol^{-1}K^{-1}$]	Heat transfer coefficient
σ	[kgs^{-2}]	Surface tension
Height	[m]	Length of column
d_P	[m]	Particle diameter
h_T	[m^3m^{-3}]	Liquid holdup
ϕ	[-]	Volume fraction
D_G	[ms^{-1}]	Diffusivity of gas
D_L	[ms^{-1}]	Diffusivity of liquid
N_{CO_2}	[$molm^{-2}s^{-1}$]	Molar flux of Carbon Dioxide in rate based model
N_{H_2O}	[$molm^{-2}s^{-1}$]	Molar flux of Water in rate based model
Sc_L	[-]	Schmidt number $\mu/\rho D_{i,L}$
Sc_G	[-]	Schmidt number $\mu/\rho D_{i,G}$
$c_{P,i}$	[$Jmol^{-1}K^{-1}$]	Molar heat capacity of liquid
C_{MEA}	[$molm^{-3}$]	Concentration of MEA

Subscript

G	Gas
L	Liquid
equilibrium	Equilibrium condition
initial, 0	Initial condition
in	Inlet
out	Outlet
CO_2	Carbon Dioxide
H_2O	Water
$MEACOO^-$	Monoethanoamine Carbamate
H_3O^+	Hydronium Ion
OH^-	Hydroxide Ion
HCO_3^-	Bicarbonate Ion
CO_3^{2-}	Carbonate Ion
CO_2, g	Carbon Dioxide in Vapour
N_2, g	Nitrogen in Vapour
H_2O, g	Water Vapour
Antoine	Using Antoine Equation
absorbed	Absorbed in the Amine
stage	Equilibrium stage

Chapter 1

Introduction

Figure 1-1 shows that since 1850, the average surface temperature has increased by approximately 0.6°C relative to the mid 20th century baseline. One of the main causes of the increase in the average surface temperature is the increase in concentration of greenhouse gases such as carbon dioxide (CO_2) whose concentration profile resembles the temperature profile.

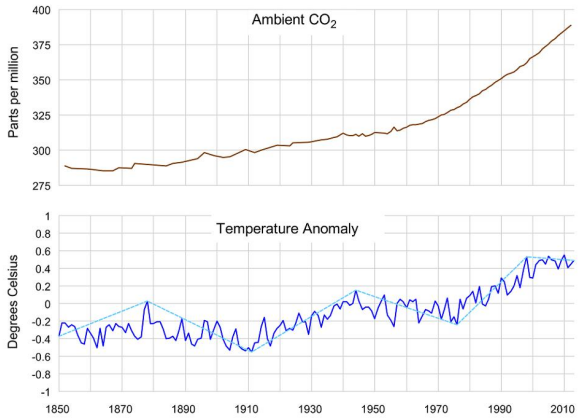

Figure 1-1: Carbon Dioxide Level and Temperature Anomaly (Metoffice.gov.uk [2016])

The increase in concentration of carbon dioxide can be attributed to the increase in energy demands of an increasing world population. According to What'sYourImpact.org [2016], 87% of all human produced carbon dioxide emissions come from the burning fossil fuels like coal, natural gas and oil. The remainder is the result of deforestation and other manufacturing process. Electricity and heat generation sectors produce the largest amount of man-made carbon dioxide emissions. This sector produced 41% of fossil fuel related carbon dioxide emissions in 2010.

One way to mitigate the rising carbon dioxide levels is by selectively capturing the carbon dioxide that is being released among the combustion products. Since, the electricity and

heat generation sectors produce 41% of the fossil fuel related carbon dioxide, it makes sense to capture it directly at those places known as point sources. Ordinarily, the combustion products of the burning fuel that are rich in carbon dioxide are released into the atmosphere. In order to absorb the carbon dioxide from the flue gas, there are a few existing methods that are commonly used. They are:

1. Membrane Absorption: A selective membrane that will allow carbon dioxide to pass through while restricting the path for other components. For this method to work properly, the partial pressure of carbon dioxide must be sufficiently high. That can be achieved either by using a stream that has a higher concentration of carbon dioxide in the flue gas stream or by increasing the pressure of the system. Additional costs need to be added to account for the cost of pressurizing the stream and the cost of increasing thickness to bear the new pressure.

2. Physical absorption: It is the process of selective absorption of an element from the gaseous stream into the bulk of the separating liquid without the occurrence of a reaction. This process also requires a higher partial pressure of the component to be removed.

3. Adsorption: It is the selective adhesion of components inside the gaseous stream onto a surface. This results in the creation of a film of adsorbate on the surface of the adsorbent

4. Chemical Absorption: This is the most commonly used and most developed technology, where a liquid chemical agent is used to selectively capture a component in the gaseous stream by reacting with it. This reaction is reversible, but the extent of its reversibility depends on the basicity of the solvent. The reaction is an acid base reaction where acidic carbon dioxide reacts with a basic solvent to form an intermediate compound. The captured carbon dioxide can be regenerated from the solvent by the application of heat. Some of the common solvents being used for chemical absorption are alkanoamines, ammonia, potassium carbonates etc. Alkanoamines such as Monoethanolamine (MEA), Diglycolamine(DGA), Diethanolamine(DEA),2-Amino-2-methyl-1-propanol(AMP), Methyl Diethanolamine(MDEA) are widely used as solvents. The method of chemical absorption using is used for modelling in this report.

The chemical absorption system consists of an absorber , a stripper, heat exchangers and pumps. The heat required to regenerate the solvent and to recover the absorbed carbon dioxide accounts for approximately 70 % of the operating costs according to Mofarahi et al. [2008]. It also accounts for 10-20 % of the initial investment. So decreasing the energy required for the regeneration8 step is essential to decrease the costs involved. There are different research areas that deal with this issue in different ways. One of them is by the choice of the solvent. As discussed previously, the basic nature of the solvent is directly correlated to the amount of energy required for regeneration. A primary amine is more basic and more reactive than a secondary amine which is more basic and reactive than a tertiary amine. A good reactivity of the amine is essential in order to absorb a large proportion of carbon dioxide from the flue gas stream. However this comes at a cost at the regeneration energy. So there needs to be a trade-off in order to select the perfect solvent. There are solvent solutions which combine multiple solvents, where a large portion of the solvent consists of a

less reactive amine such as MDEA and a small portion consists of a highly reactive amine such as Piperazine (PZ).

One of the unique solutions that Technip has come up with along with ECN and others is Heat Integrated Distillation for absorption. Heat-integrated distillation (HIDIC) is a concept dating back to the 1980's which shows a large potential for energy savings in the operation of distillation columns in the chemical industry. Case studies have shown up to 80% primary energy reduction. Despite the large energy savings, the complexity of the technology hinders the implementation of heat-integrated distillation. This HIDIC design is based on a plate-fin heat exchanger(PFHE) which consists of parallel flat plates with corrugated fins. The PFHE is arranged for parallel vertical flows in alternating stripper and rectifier layers. In each layer there is a counter current flow of gas and liquid with liquid flowing downwards as a film on the walls.

The initial aim of this project was to model the mass transport and heat transport involved in both the regular and HIDIC absorption processes. In order to model the HIDIC equipment, it was required to make an equation based model of the regular column where the equations are written in residual form. The advantage of having an equation based model is that the modeller / user has the option to decide which variables need to be considered and what parameters could be relevant. A verified model of the conventional absorber can be used in the next stage to model the HIDIC column. Furthermore, Technip is interested to study the impact of the temperature bulge on the absorption column. So, it was important to know if the proposed model can predict the bulge and to understand what factors affect the shape and position of the bulge. Two different models were proposed in this study which represent the two existing approaches for chemical absorption modelling. They are the **Rate Based Model** and the **Equilibrium Model**.

1-1 Outline

The different processes that occur during chemical absorption are explained in chapter 2. Furthermore, it also contains the concepts and approaches that are used in the development of a mathematical model.

The equilibrium and rate based models are presented in chapter 3.

The results of both the models are reported in chapter 4. First, the equilibrium model is validated against the model of Mores et al. [2012] and the rate based model is validated against the model of Simon et al. [2011]. This validation is done in order to check if the models are implemented properly. Next, in order to select the more accurate model, a series of 4 tests are conducted with different conditions to check if the predictions of the models match the experimental data. Lastly, an analysis of the factors that affect the temperature bulge is presented.

The conclusions summarizing the findings of the work can be found in chapter 5.

Chapter 2

Theory

2-1 Absorption Column

The equipment in which carbon dioxide is absorbed into the separating liquid is known as an absorption column. The separating liquid used in this thesis is **Monoethanolamine (MEA)**. The choice of the separating liquid was due to convenience. The physical and chemical properties of MEA are available openly in science journals. However, the equations of both the models can be used with other amines provided the properties are available.

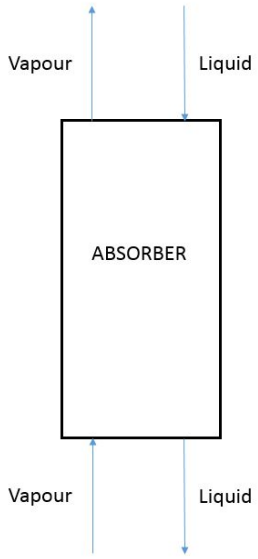

Figure 2-1: Symbolic Representation of an Absorption Column

Figure 2-1 shows a symbolic representation of an absorption column. MEA solution is introduced at the top of the column, while the flue gas is introduced at the bottom of the

column. As the amine solution flows downwards along the column, it reacts with carbon dioxide in the gas stream and sets off a set of parallel reactions that end up storing carbon dioxide as an intermediate compound. The amine solution at the outlet i.e. bottom of the column, has a significantly higher concentration of carbon dioxide than at the top of the column and is known as **rich amine**. The amount of carbon dioxide which is captured by the amine solution is calculated by a variable (α) which is known as loading. The captured carbon dioxide is stored as bicarbonates, carbonates, carbamates and dissolved carbon dioxide. The loading of the amine can be defined as a ratio of the moles of captured carbon dioxide to the moles of the MEA at the inlet. While denominator of this ratio remains constant, the numerator or captured carbon dioxide keeps on increasing till its maximum value. The concentration of water inside the solution is much greater than concentration of amine. The solution on contact with the flue gas tries to saturate it in order to achieve vapour liquid equilibrium . This process which takes place simultaneously with the absorption, produces either evaporation or condensation depending on the amount of water vapour in the flue gas stream. Both these processes are accompanied by a transfer of energy from one phase to another which result in either heating or cooling of the liquid stream.

The absorption process is always followed by the stripping process in order to recover the solvent and to regenerate the absorbed carbon dioxide. In this process, the rich amine solution is sent to the stripper where the addition of heat reverses the reactions that occurred in the absorption column and results in a release of carbon dioxide. This amine is known as the **lean amine**, as most of the absorbed carbon dioxide is removed by the addition of heat. Complete recovery of the absorbed carbon dioxide is not possible and there is always a small portion of carbon dioxide which is left inside the amine solution. The recovered amine is sent to the top of the absorption column as the lean amine where the cycle continues.

The complex dynamics that are occurring inside the absorption column need to be captured in a robust mathematical model. Two approaches are available in literature, they are **Equilibrium** and **Non Equilibrium** approach. These approaches are discussed in the following sections.

2-2 Equilibrium Approach

The core principle of the equilibrium approach is the assumption that the vapour and liquid streams are in thermodynamic equilibrium with each other. These models essentially use the **MESH** equations.

1. **M**: Material Balance Equation.
2. **E**: Equilibrium relations between the outlet liquid and vapour.
3. **S**: Summation of mole fractions is equal to one.
4. **H**: Heat Balance: The energy / enthalpy balance to signify that energy is conserved.

The MESH equation approach is commonly used to model a Distillation column. But, the process of absorption is significantly different than the process of distillation. Namely, in

addition to the MESH equations, the model has to account for the parallel reactions that occur simultaneously. The presence of reaction renders some of the MESH equations obsolete in their original form. For example, due to production of species in the reactions, the species balance equation (2-21) in its original form has to be altered to account for the production or consumption of species. These reactions are assumed to be in equilibrium. Also additional equations such as charge balance, solvent balance, carbon capture equation etc. have to be added.

In reality the concept of complete thermodynamic equilibrium between the two streams is inaccurate. This problem is partially solved by assuming an efficiency which accounts for the non ideality of the process. One of the most common efficiencies used for the distillation column calculations is known as the **Murphree efficiency**. This efficiency is only applicable in cases where vapour, liquid are completely mixed. It is defined for each tray or stage according to the extent of separation achieved. According to Process [2016], it is defined as the ratio of the change in actual concentration to the change predicted by the equilibrium condition. This parameter has a unique value for each component in each stage of the column. For new processes, this value is unknown.

2-3 Rate Based Approach

Rate Based models treat the separation process to be governed by mass and heat transfer phenomena. The mass transfer rate is proportional to the difference in concentrations of a component at two different locations. This implicitly assumes that the vapour and liquid are not in thermodynamic equilibrium and the extent to which they are not in equilibrium with each other will drive the process of heat and mass transfer. The rate based models usually use the **MERSHQ** equations as formulated by Taylor and Krishna [1993].

1. **M**: Material/Mass conservation equation.
2. **E**: Energy conservation equation
3. **R**: Mass/ Heat transfer rates
4. **S**: Summation of mole fractions
5. **H**: Pressure drop equations
6. **Q**: Equilibrium relations

Separate balance equations are written for each distinct phase which is completely different to the equilibrium approach where it was possible to write the material balances of both phases together. This method involves the detailed description of the heat and mass transfer rates which generally results in a system of ordinary or partial differential equations. The two phases are assumed to be at equilibrium only at the interface.

2-4 Reactions

A set of parallel reactions are set off when the flue gas gets into contact with the amine solution. The amine solution consists of MEA and water. MEA is a primary amine with a chemical formula of $HO-CH2-CH2-NH2$ which is commonly used for its fast reaction with carbon dioxide. The first process that takes place is the dissolving of the vapour carbon dioxide in the liquid solution and evaporation/condensation of water depending on the saturation pressure. This is described by the equation 2-9 and 2-10. Next, a set of instantaneous reactions are set off due to presence of dissolved carbon dioxide in the amine. They include the ionization of water as shown in equation 2-1, dissolving of carbon dioxide in water to form carbonic acid, shown in equation 2-2, dissociation of bicarbonate, shown in equation 2-3, dissociation of protonated MEA, shown in equation 2-4 and carbamate reverting to bicarbonate due to hydrolysis, shown in equation 2-5.

The overall reaction between monoethanolamine and carbon dioxide is listed in equation 2-8. There exist different theories on the reaction mechanism and one of the common ones used is the zwitterion mechanism. A zwitterion can be defined as a complex molecule with both positive and negative charges. The formation of zwitterion is shown in equation 2-6 and its deprotonation is shown in equation 2-7. The deprotonation is much faster than the zwitterion formation and therefore the formation of zwitterion is considered the rate limiting step for the overall reaction

Chemical Absorption

$$2H_2O \longleftrightarrow H_3O^+ + OH^- \tag{2-1}$$

$$2H_2O + CO_2 \longleftrightarrow H_3O^+ + HCO_3^- \tag{2-2}$$

$$H_2O + HCO_3^- \longleftrightarrow H_3O^+ + CO_3^{2-} \tag{2-3}$$

$$H_2O + MEAH^+ \longleftrightarrow H_3O^+ + MEA \tag{2-4}$$

$$MEACOO^- + H_2O \longleftrightarrow MEA + HCO_3^- \tag{2-5}$$

Zwitterion formation and Deprotonation

$$CO_2 + MEA \longleftrightarrow MEA^+COO^- \tag{2-6}$$

$$MEA + MEA^+COO^- \longleftrightarrow MEAH^+ + MEACOO^- \tag{2-7}$$

Overall Reaction

$$CO_2 + 2MEA \longleftrightarrow MEAH^+ + MEACOO^- \tag{2-8}$$

Physical Absorption

$$CO_2(aq) \longleftrightarrow CO_2(gas) \tag{2-9}$$

$$H_2O(aq) \longleftrightarrow H_2O(gas) \tag{2-10}$$

The challenging aspect of modelling a reactive absorption system is to account for these reactions in the mathematical model. There are different ways to include the effect of the above mentioned reactions in the mathematical model. They are:

- Chemical Equilibrium

- Rate of Reaction
- Enhancement Factors
- Extent of Reaction

2-4-1 Chemical Equilibrium

This method is used in various equilibrium models such as Mofarahi et al. [2008], Mores et al. [2012] etc. The basic premise of this approach is that for instantaneous reactions such as reaction 2-11, the concentrations of the components are related by the definition of the equilibrium constant i.e. equation 2-12. These parallel reactions are written in the form of a residual and combined with other MESH equations to give a larger set of equations that must be solved together.

$$aA + bB \longleftrightarrow cC + dD \tag{2-11}$$

$$\mathrm{K_{reaction}} = \frac{\gamma_c \mathrm{x_c} \gamma_d \mathrm{x_d}}{\gamma_a \mathrm{x_a} \gamma_b \mathrm{x_b}} = \frac{C_C^c C_D^d}{C_A^a C_B^b} \tag{2-12}$$

2-4-2 Rate of Reaction

Another way of incorporating the reaction is by considering the forward and backward rate of reaction. These rates of generation / consumption of a species can be added to the overall conservation equation for each component. Take the case of reaction 2-13, which lists the conservation equation of a component i. R denotes the overall rate of reaction.

$$\frac{\mathrm{dC_i^l}}{\mathrm{dt}} = -\mathrm{u_l}\frac{\partial \mathrm{C_i^l}}{\partial \mathrm{z}} - \mathrm{n_{i,diffusion}} + \mathrm{R_{i,reaction}} \tag{2-13}$$

It is used in Greer [2008], Kucka et al. [2003], Kvamsdal et al. [2009] etc. The reaction rate can be applied for the liquid film in the two film theory or the entire liquid phase.

2-4-3 Enhancement Factors

Enhancement factor (E) can be defined according to equation 2-14. It numerically describes the increased diffusion due to the presence of reactions.

$$\mathrm{E} = \frac{\text{Diffusion Rate with reaction}}{\text{Diffusion Rate without reaction}} \tag{2-14}$$

The enhancement factor is applied in the model by multiplying it to the component whose diffusion rates are supposed to be enhanced with the presence of reactions i.e. carbon dioxide.

$$\mathrm{N} = \mathrm{Ek_l}(\mathrm{C_{i,Interface}} - \mathrm{C_{i,Bulk}}) \tag{2-15}$$

A large number of correlations exist for calculating enhancement factors based on different mass transfer models. The correlation of Cussler [2009] is ultimately used in the rate based model but other correlations are tested in appendix 6-7.

For calculating the enhancement factor, the essential properties required are the rate constant of the rate controlling reaction in the amine process i.e. equation 2-6, Diffusivity of carbon dioxide in the amine, concentration of amine in the solution and the liquid mass transfer coefficient. A dimensionless constant known as the Hatta number needs to be calculated first. It is defined as the ratio of the maximum rate of reaction in the liquid film to the maximum rate of mass transfer through the liquid film. Depending on the mass transfer model chosen, the Hatta number is used to calculate the enhancement factor. This method of calculating the enhanced effect of reactions on the mass transfer by the means of an Enhancement Factor is used by d by Gabrielsen et al. [2006], Kvamsdal et al. [2009] , Greer [2008] etc.

2-4-4 Extent of Reaction

Equilibrium concentrations can also be calculated by calculating the percentage of reactants that are converted to the products at thermodynamic equilibrium. This is known as the extent of reaction approach. Consider reaction 2-16, if an infinitesimal amount (ξ) of reactant A is converted into the product B. The extent of reaction is defined in equation 2-17, where $\mathrm{n_i}$ refers to the number of moles of the i^{th} component and ν refers to the stoichiometric number of that component.

$$aA \longleftrightarrow bB \tag{2-16}$$

$$\xi = \frac{\mathrm{dn_i}}{\nu} = \frac{\Delta \mathrm{n_A}}{\mathrm{a}} \tag{2-17}$$

$$\xi = \frac{\mathrm{n_{i,equilibrium}} - \mathrm{n_{i,initial}}}{\nu} \tag{2-18}$$

For a component involved in multiple reactions,

$$\mathrm{n_{i,equilibrium}} = \mathrm{n_{i,initial}} + \sum_{\mathrm{j=1}}^{\mathrm{Reactions}} \nu_\mathrm{i}\xi_\mathrm{j} \tag{2-19}$$

If the equation is properly balanced and the initial amounts of the reactants and products are known, then equation 2-19 can be used to determine the equilibrium concentration. This set of equations can be added to the existing set of mass, material and energy balances.

2-5 Mass Transfer

Mass transfer is defined as the net movement of mass from one location to another. The driving force for this phenomena in an absorption column is the difference in chemical potential. A chemical species will move from areas of high chemical potential to areas of low chemical potential.

According to Processes [2016], Gas absorption can be defined as an operation in which a gas mixture is contacted with a liquid for the purpose of preferentially dissolving one or more components of the gas mixture and to provide a solution of them in the liquid. For gas absorption, there are a few existing models which describe the mass transfer such as two film model, surface renewal model, penetration theory etc. The two film model is used in the rate based model. In this model, the liquid and vapour films are placed next to each other as shown in figure 2-2. The two-film model assumes that the entire resistance to mass transfer is concentrated in the two films.

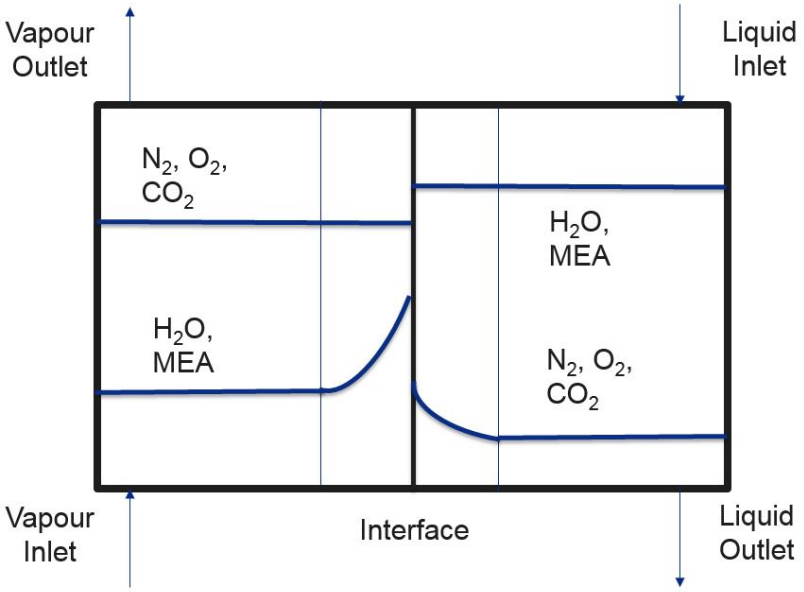

Figure 2-2: Concentration gradients of two film theory for CO_2 absorption in MEA

According to Taylor and Krishna [1993], the mass transfer only takes place due to steady state molecular diffusion. The difference in concentration generates the driving force necessary to drive the mass transfer. Vapour and liquid are at equilibrium only at the interface of these two films. The bulk of the liquid and vapour streams are assumed to have constant concentrations.

There are different theoretical relations that can accurately depict diffusion which are explained in Taylor and Krishna [1993]. The most rigorous of these correlations is known as the Maxwell-Stefan relation, in which the diffusion fluxes are related to the electrical and potential gradients. These relations can be simplified to the Fick's law for vapour and Nernst-Planck equation for liquid. If convective mass transfer and the effect of electric potential is neglected, the end result is the simplified Fick's law (equation 2-20) which is used in this thesis.

$$J = -D\frac{dC}{dx} \tag{2-20}$$

where J is diffusion flux. D is the diffusion coefficient. C is the concentration

2-5-1 Mass Transfer Coefficient

According to Fick's Law equation 2-20, the diffusion flux is directly proportional to the concentration difference.The proportionality constant is known as the mass transfer coefficient. It can also be defined as the diffusion coefficient per unit length. The mass transfer coefficient is estimated by using correlations that exist in literature. It is a function of density, viscosity, diffusivity etc. The accurate calculation of the mass transfer coefficient is essential for the model to calculate the amount of diffusion.

Billet and Schultes [1999] and Onda et al. [1968] are commonly used for carbon dioxide amine absorption as well as other phenomena. A detailed review of mass transfer coefficients is listed in Wang et al. [2005]. There is no universally accepted mass transfer coefficient correlation which can be used in each and every case. Heat transfer is happening simultaneously along with the mass transfer. The heat flux is directly proportional to the temperature difference and the constant of proportionality is known as the heat transfer coefficient. The Chilton - Colburn analogy is used in order to calculate the heat transfer coefficient. This analogy relates the heat transfer coefficient to the mass transfer coefficient and friction factors. Equation 3-38 shows the correlation which is used in the rate based model.

2-5-2 Interfacial Area

Effective interfacial area approximates the area that is available where two-phases can come into contact. This quantity is used to calculate the amount of flux that is being transferred upon contact. Accurate estimation is crucial to calculate the area of contact between liquid and vapour. It is denoted by the symbol 'a_w'. Billet and Schultes [1999] and Onda et al. [1968] correlations for interfacial area are commonly used. A larger list is compiled with other correlations and is presented in Wang et al. [2005]. A common assumption that is taken into account is that the area of contact for mass transfer and heat transfer are the same. This assumption has been used in the rate based model.

2-6 Temperature Profile

The absorption of carbon dioxide into the amine releases energy and heats up the liquid stream, while evaporation of water from the amine solution absorbs energy and cools the liquid stream. Other processes such as heating up of both the streams and heat loss to the environment add to the complexity of the system. These simultaneous processes result in the liquid stream having different temperatures at different locations inside the absorption column which is known as the temperature profile. Sometimes, the temperature of the liquid stream inside the column is larger than its temperature at the inlet and the outlet. This phenomena is known as the 'Temperature Bulge'. With an increase of temperature inside the column, the equilibrium solubility of carbon dioxide is decreased which affects the extent of absorption. This phenomena of the temperature bulge is of interest to Technip.

2-7 Models Reviewed

The models that were reviewed in order to understand the concepts behind modelling reactive absorption are explained in this section.

First, the equilibrium models of Mofarahi et al. [2008] and Mores et al. [2012] were reviewed. As mentioned previously, the basic structure of the equilibrium is a system of MESH equations onto which the chemical reactions are added. Consider the equilibrium model proposed by Mofarahi et al. [2008], it only considers carbon dioxide to be involved in vapour liquid equilibrium and neglects the condensation/ evaporation of water. A Murphree efficiency of 35% is used by the authors to account for the non-ideality of the process. This model combines the material balances, Murphree efficiency equation, energy equation, charge balance, vapour liquid equilibrium for carbon dioxide, 5 parallel reactions that are considered to be at equilibrium. The model provided the basic structure for an equilibrium model but was unclear on its implementation. The source of this confusion is the usage of the loading variable or 'α'. This variable captures the amount of carbon dioxide which is captured by the amine. The mathematical model listed its value as a parametric function which would be independent of the concentrations of the inlet streams. This is incorrect as the loading of amine is dependent on the amount of carbon dioxide absorbed which obviously depends on the concentrations of both the liquid and the gas stream. Additionally, there were incorrect equations and incomplete information which caused a delay in the project for the author.

A similar equilibrium model was proposed by Mores et al. [2012] with some changes. One of the most important change was considering water to be involved in the vapour liquid equilibrium with carbon dioxide. This model also accounts for the non ideality of the absorption process by using the Murphree efficiency values of 0.3 and 0.4. The changes presented in Mores et al. [2012] made the equilibrium model more accurate than the model of Mofarahi et al. [2008]. However, it had a few errors which had to be corrected to prepare an accurate equilibrium model. Specifically, the overall mass balance of Mores et al. [2012] is shown as in equation 2-21 where j refers to the stage number.

$$L_J - L_{J+1} + G_J - G_{J-1} \tag{2-21}$$

Where L and V are mole flow rates. The problem with this equation is that a mole balance is not possible when there is generation of moles from a reaction. This equation can be altered by adding a generation term. Additionally, the way reactions were incorporated in the model was not completely clear. It appeared that the model was using mole fractions for the definition of the equilibrium constant which were multiplied by the activity coefficients. This model was used as a basis of making the equilibrium model and the errors that were discovered in the literature review were addressed.

After the selection of the equilibrium models, the next step is to choose a rate based model. The models of Khan et al. [2011], Kucka et al. [2003], Al-Baghli et al. [2001], Kvamsdal et al. [2009], Greer [2008] and Gabrielsen et al. [2006] were reviewed.

Gabrielsen et al. [2006] proposed a steady state rate based model to model the carbon dioxide - AMP system which was based on the material and energy balances that was developed by Pandya [1983]. This system of balance is presented as a system of Ordinary Differential equations (ODE). The molar fluxes of carbon dioxide and water from liquid to vapour and

vice versa, were the main variables in this system. By using these variables, the model accounted for the transfer of moles from one phase to the other. The carbon dioxide flux from the vapour stream to the liquid stream needs to account for the presence of reactions. This is done by utilizing an enhancement factor which quantifies the increase in mass transfer due to reactions. The model was developed in Matlab^{TM}. Models such as Simon et al. [2011], Faramarzi et al. [2010], Afkhamipour and Mofarahi [2013] also following a similar approach. Although the structure of the model was very simple and easily modifiable, it did not clearly state all the equations that were being used in their proper form. For example, in Simon et al. [2011] and Gabrielsen et al. [2006], the overall mass transfer coefficient for gas shown to be defined by the equation 2-22. In this equation k_L and k_G are taken from Billet and Schultes [1999] whose units are [ms^{-1}]. This equation is derived from the two film theory in which the Henry's constant is supposed to be dimensionless. But in its use in this model, the units of Henry's constant are [Pam^3mol^{-1}]. So the units of the gaseous mass transfer coefficient must be changed so as to be able to be used in this equation. Specifically, the units of the mass transfer coefficients are altered in all these papers by dividing the original mass transfer coefficient by RT_G as shown in equation 3-29. But, since this information is not disclosed, chances of errors increase.

$$\frac{1}{K_G} = \frac{1}{k_G} + \frac{H_{CO_2}}{Ek_L} \tag{2-22}$$

Khan et al. [2011] proposed a steady state rate based model which assumes that the solvent does not evaporate. A similar system of ODE's is developed which considers The effect of reactions is captured by the use of enhancement factor approach. The model is solved using a shooting method in Excel [2013]. This model is validated by comparing the results to a few experiments including the one from Tontiwachwuthikul et al. [1992]. He also performs a sensitivity analysis of the model to check the influence of mass transfer relations on the results which lead him to conclude that the relations from Onda et al. [1968] give the most accurate results.

Kucka et al. [2003] proposed a steady state model based on two film theory which considers the effect of reaction without the simplified enhancement factor concept. This model sets up equation in the axial direction i.e. along the column and also a different set of equations for the film. Aspen Custom (AspenTech [2013]) modeller was used to model the equations. Billet and Schultes [1999] was used for mass transfer coefficient. It was validated against the experiment of Tontiwachwuthikul et al. [1992]. Sensitivity analysis was performed by testing different kinetic descriptions which shows significant deviation in the calculation up to 17 %. The advantage of using this model is that the concentration profiles along the film can provide extra information which can't be achieved by models which integrate only along the column. Another model which incorporates the rigorous film dynamics is the model of Al-Baghli et al. [2001]. He proposed a model that is based on two film theory where the enhancement factor is calculated by solving 5 differential equations of 5 major components instead of using a simplified expression or correlation. Reactions are assumed to take place only in the liquid film.

Kvamsdal et al. [2009] proposed a dynamic model based on two film theory which was solved in gProms. Both carbon dioxide and H_2O are assumed to go across the interface depending on the driving force of the concentration gradient. The reactions are taken into account by their effect on the mass flux / mass transfer in the form of an enhancement factor which was calculated by using the equilibrium model of Hoff [2003]. The liquid velocity is assumed to

be constant but gas velocity is assumed to be a variable. The mass transfer coefficients of Onda et al. [1968] are used.

Greer [2008] proposed a dynamic model of a carbon dioxide absorption system which consisted of a model of the absorber, stripper, heat exchangers etc. This model incorporated the effects of reaction in the form as shown in section 2-4-2. This model was developed in Matlab^{TM}. The advantage of this model was that it could be easily adapted for any other amine and could be used in other platforms such as Python^{TM}. The absorber model was isolated and implemented by the author but it was consistently under predicting the amount of absorption under steady state conditions.

Finally after comparing the models and knowing that the platform had to be implemented in Python^{TM}. The model of Gabrielsen et al. [2006] was chosen to be the rate based model which had to be modified for usage for MEA.

Chapter 3

Models

3-1 Equilibrium Model

An equilibrium model is proposed for the design of an absorption column using MEA solution. The absorption column is assumed to be divided into stages by the use of trays. A model is made for a random stage in the column as shown in figure 3-1. Each stage has vapour and liquid as inlets entering the stage in opposite directions. It has two outlet streams.

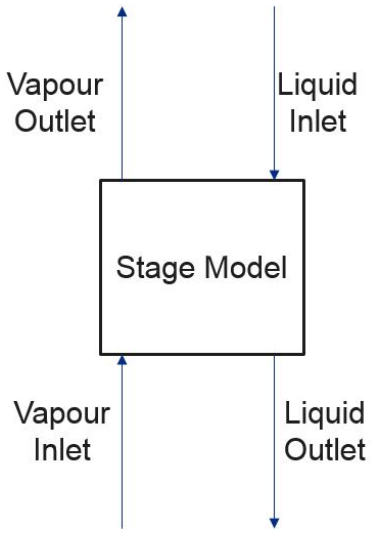

Figure 3-1: Symbolic representation of a general stage of an **Equilibrium Model**

The assumptions for this model are:

- The pressure is constant.

- All the reactions are at equilibrium.
- The outlet streams are in thermodynamic equilibrium with each other.
- Water and carbon dioxide are the only components that can change phase.
- Adiabatic column.
- Henry's law is used to calculate equilibrium carbon dioxide solubility.
- Antoine equation is used to give the vapour pressure of water.

3-1-1 Mathematical Model

The reactions 2-1-2-5 are used in the equilibrium model. The model assumes that all the reactions reach equilibrium instantaneously and the equilibrium concentrations can be calculated by using the equilibrium constant. The concentration of water is assumed to be constant since its concentration is much greater than the concentration of all the other chemical species. This approach is taken from the paper of Aboudheir et al. [2003], which also provides the chemical equilibrium constants for this model. These values can be found in Appendix 6-2.

$$\mathrm{K1} = [\mathrm{H_3O^+}][\mathrm{OH^-}] \tag{3-1}$$

$$\mathrm{K2} = \frac{[\mathrm{HCO_3^-}][\mathrm{H_3O^+}]}{[\mathrm{CO_2}]} \tag{3-2}$$

$$\mathrm{K3} = \frac{[\mathrm{CO_3^{2-}}[\mathrm{H_3O^+}]}{[\mathrm{HCO_3^-}]} \tag{3-3}$$

$$\mathrm{K4} = \frac{[\mathrm{MEA}][\mathrm{HCO_3^-}]}{[\mathrm{MEACOO^-}]} \tag{3-4}$$

$$\mathrm{K5} = \frac{[\mathrm{MEA}][\mathrm{H_3O^+}]}{[\mathrm{MEAH^+}]} \tag{3-5}$$

A specified number of moles of MEA or $\mathrm{N_{MEA_0}}$ enters the top of the column. At equilibrium, the inlet amine effectively splits up to form $\mathrm{MEACOO^-}$ and $\mathrm{MEAH^+}$. The remaining number of moles of amine which have not reacted is denoted by $\mathrm{N_{MEA}}$. This process is mathematically explained in equation 3-6. The amount of carbon dioxide caught by the amine is denoted by the variable α which is also the input to the system. It is known as mole loading of the amine and it is defined as the ratio of moles of absorbed carbon dioxide to the moles of inlet amine. The absorbed carbon dioxide exists inside the amine as aqueous $\mathrm{CO_2}$, $\mathrm{MEACOO^-}$, $\mathrm{CO_3^{2-}}$ and $\mathrm{HCO_3^-}$, which is shown in the equation 3-7. Due to the production of ionic species such as $\mathrm{MEACOO^-}$, $\mathrm{CO_3^{2-}}$ etc. during absorption, an assumption is made in the model which states that the positively and negatively charged species which are formed due to dissociation and reactions will balance each other to give an electrically neutral solution. This concept is denoted by equation 3-8. The current system has 8 species, 6 ions and 2 neutral molecules. Another equation was required to calculate the moles of water in the solution. To solve this problem, an oxygen balance equation is proposed in equation 3-9. It states that the amount of oxygen that exists in the system in the form of ions or neutral molecules such as $\mathrm{CO_2}$ or

H_2O is equal to the amount of oxygen which is present in the incoming water added to the amount of oxygen which is captured by the amine in the form of carbon dioxide.

$$N_{MEA} + N_{MEAH^+} + N_{MEACOO^-} = N_{MEA_0} \tag{3-6}$$

$$N_{CO_2} + N_{HCO_3^-} + N_{CO_3^{2-}} + N_{MEACOO^-} = \alpha N_{MEA_0} \tag{3-7}$$

$$N_{MEAH^+} + N_{H_3O^+} = N_{HCO_3^-} + N_{OH^-} + 2N_{CO_3^{2-}} + N_{MEACOO^-} \tag{3-8}$$

$$2N_{CO_2} + N_{H_2O} + N_{MEACOO^-} + 2N_{H_3O^+} + N_{OH^-} + 3N_{HCO_3^-} + 3N_{CO_3^{2-}} = 2\alpha N_{MEA_0} + N_{H_2O_0} \tag{3-9}$$

As stated previously, only water and carbon dioxide can change phases. For water vapour, the driving force for the change of phase is the difference between the equilibrium vapour pressure and the actual partial pressure of the water vapour. The equilibrium vapour pressure of water is calculated by using the Antoine's equation whose coefficients are provided in table 6-2. The equilibrium vapour pressure is used in the Raoult's law equation 3-10 to calculate the moles of water vapour.

Equation 3-11 fixes the pressure of the gaseous components inside a stage. The gaseous components used in this report are CO_2, H_2O and N_2. But the model can be easily modified to model any gas stream, by adding new variables for the non reactive components and equations such as equation 3-13. The number of moles of carbon dioxide captured by the amine is defined by the equation 3-12. Furthermore, equation 3-14 establishes a link between absorbed, inlet and outlet carbon dioxide.

Murphree efficiency is used to account for the non ideality of the system in this model. It affects the partial pressure of the carbon dioxide vapour as shown in equation 3-18. The denominator in equation 3-18 defines the maximum possible absorption and the numerator defines the real amount of absorption taking place in this system.

Finally, the energy equation 3-17 is required to calculate the temperature of each stage. AspenTech [2013] correlations are used to calculate the specific heats of gaseous components and Weiland et al. [1997] correlations are used to calculate the specific heat for the amine solution. Gabrielsen et al. [2006] correlation is used for calculating the heat of absorption of carbon dioxide inside the amine and EngineeringToolbox.com [2016] is used to calculate heat of evaporation/condensation of water.

$$P_{H_2O_g} = P_{H2O,Antoine} * x_{H_2O} \tag{3-10}$$

$$P_{CO_{2g}} + P_{N_{2g}} + P_{H_2O_g} = P_{stage} \tag{3-11}$$

$$N_{CO_{2absorbed}} = (\alpha - \alpha_{in}) N_{MEA_0} \tag{3-12}$$

$$N_{N_{2g,out}} = N_{N_{2g,in}} \tag{3-13}$$

$$N_{CO_{2in}} = N_{CO_{2absorbed}} + N_{CO_2} \tag{3-14}$$

$$P_{N_{2g}} = y_{N_2} P_{stage} \tag{3-15}$$

$$P_{H_2O_g} = y_{H_2O} P_{stage} \tag{3-16}$$

$$H_{l,in} - H_{l,out} + H_{g,in} - H_{g,out} + \Delta H_{CO_2} - \Delta H_{H_2O} = 0 \tag{3-17}$$

$$\eta_{murphree} = \frac{P_{CO_{2g}} - P_{CO_{2g,in}}}{He[CO_2] - P_{CO_{2g,in}}} \tag{3-18}$$

3-1-2 Inlet Conditions

In order to be able to run this model for any condition, the user needs to know the following:

1. Composition of liquid stream. The inlet moles of water and amine are required. Additionally the loading is used to determine the concentration of all the ions in the liquid.
2. Composition of vapour stream in moles. This includes the inlet moles of vapour components such as H_2O, N_2 and CO_2.
3. Liquid stream temperature [K]
4. Vapour stream temperature [K]

3-1-3 Multi Stage

The multi stage column is made by cascading a fixed number of stages over one other as shown in figure 3-2. The stage model is defined in a way that it becomes easy to connect these stages models in series. The outlet vapour variable of the stage 3 in figure 3-2 is equal to the inlet vapour variable of stage 2 and similarly, the outlet liquid variable of stage 1 in figure 3-2 is equal to the inlet variable of stage 2. The boundary condition for the liquid stream is mentioned at the top of the column whereas it is mentioned at the bottom of the column for the vapour stream.

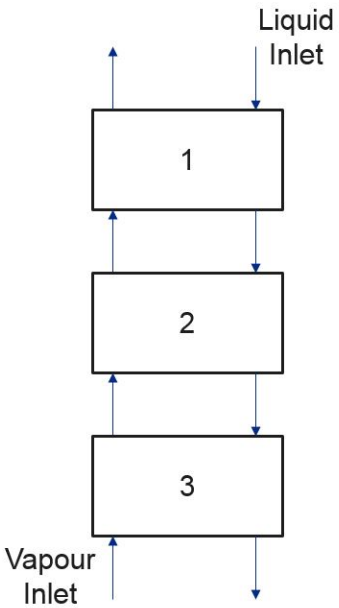

Figure 3-2: Symbolic representation of a Multi Stage column

3-1-4 Model Implementation

The model is implemented in Python^{TM}. The molar volume at each temperature is first calculated which is used to calculate all the concentrations of the liquid components. These concentrations are used in equations 3-1-3-5. The moles of the ions such as $MEACOO^{-}$, $MEAH^{+}$ etc. are actually dependent only on the moles of the inlet amine at the top of the column which is a constant and the loading in each stage which is a variable. The amount of CO_2 absorbed depends on equations 3-18 and 3-12. A function is made which returns the residuals of these equations. An in-house non linear algebraic equation solver tp_fsolve is used to solve this function. This solver requires an initial guess to calculate all the variables.

3-2 Rate Based Model

The mathematical model proposed by Gabrielsen et al. [2006] which was developed in Matlab^{TM} for the design of a packed absorber columns using the 2-Amino-2-methyl-1-propanol (AMP) solution is adopted and modified for the design of the absorption column using MEA solution. This model is developed in Python^{TM}. The main assumptions of this model are:

- Two film theory is used for modelling mass transfer.
- All the reactions only happen inside the liquid film.
- The region outside the two films (known as liquid and gas bulk) as shown in figure 2-2 are in equilibrium and do not participate in the reaction.
- The direction of the flux of carbon dioxide and water is normal to the axis of the absorption column.
- Heat loss to the atmosphere is not considered in this model.
- The effective interfacial surface is considered to be the same for both heat and mass transfer.

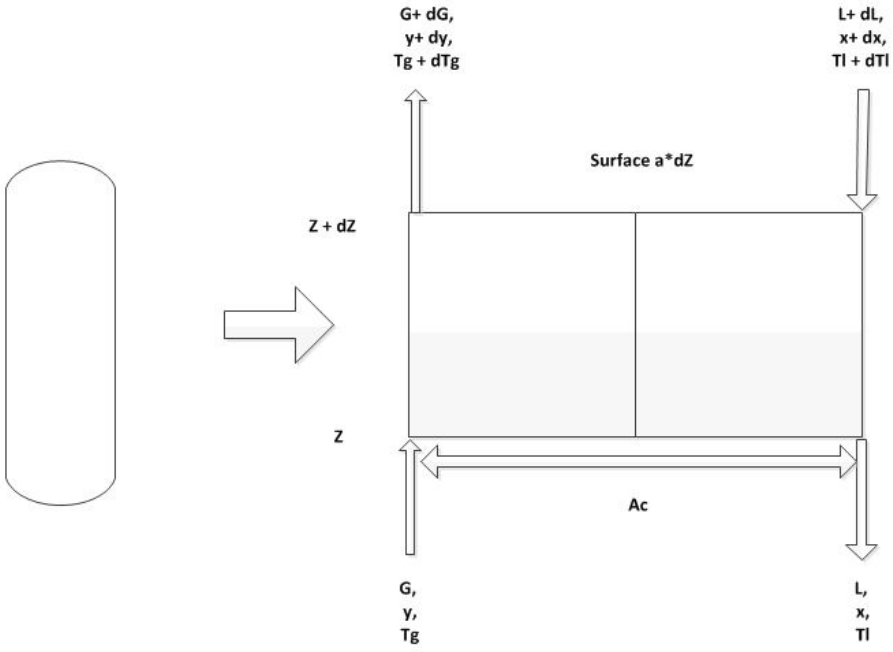

Figure 3-3: Differential Element of a Packed Column

Consider a differential element shown in figure 3-3. Flue gas with a molar flow rate of G mole/s and temperature T_g enters the column with a composition of y_i. Counter-currently,

the amine solution with a molar flow rate of L mole/s and temperature of T_l enters the column with a composition of x_i. These variables change by an infinitesimal amount over the differential element. The change in these quantities are described by the differential equations 3-19 to 3-26. These equations are based on the material and energy balance equation that were developed by Pandya [1983] who then developed an iterative procedure to solve them. Those equations were slightly modified to be used for AMP in Matlab^{TM} by Gabrielsen et al. [2006].

$$\frac{dG}{dz} = -(N_{CO_2} + N_{H_2O})a_w A_c \tag{3-19}$$

$$\frac{dy_{CO_2}}{dz} = \frac{N_{CO_2}a_w A_c(y_{CO_2} - 1) + N_{H_2O}y_{CO_2}a_w A_c)}{G} \tag{3-20}$$

$$\frac{dy_{H_2O}}{dz} = \frac{N_{H_2O}a_w A_c(y_{H_2O} - 1) + N_{CO_2}y_{H_2O}a_w A_c}{G} \tag{3-21}$$

$$\frac{dL}{dz} = -N_{H_2O}a_w A_C \tag{3-22}$$

$$\frac{dX_{CO_2}}{dz} = \frac{(N_{H_2O}X_{CO_2} - N_{CO_2})a_w A_C}{L} \tag{3-23}$$

$$\frac{dx_{H_2O}}{dz} = \frac{[N_{H_2O}(x_{H_2O} - 1) + N_{CO_2}]a_w A_C}{L} \tag{3-24}$$

$$\frac{dT_G}{dz} = -\frac{qa_w A_C}{Gc_{p,G}} \tag{3-25}$$

$$\frac{dT_L}{dz} = \frac{N_{CO_2}c_{p,CO_2} + N_{H_2O}c_{p,H_2O}a_w A_C(T_L - T_G)}{Lc_{p,L}} - \frac{qa_w A_c}{Lc_{p,L}} + \frac{(N_{CO_2}\Delta H_{CO_2} + N_{H_2O}\Delta H_{H_2O})a_w A_c}{Lc_{p,L}} \tag{3-26}$$

3-2-1 Heat and Mass Transfer

The most important component in the above equations are the interfacial fluxes of water and carbon dioxide that are being calculated by the equation 3-27. P_i^* is the partial pressure of a component in the gas phase assumed to be in equilibrium with the liquid phase. $P_{CO_2}^*$ is calculated by using a combined Henry's law and chemical equilibrium constant proposed by Gabrielsen et al. [2006]. $P_{H_2O}^*$ is calculated by using Antoine's equation. The difference between actual partial pressure (P_i) and P_i^* drives the process of molecular diffusion. The two films create a resistance to the free movement of the molecules and this resistance is mathematically captured by using the variable of mass transfer coefficient. For carbon dioxide, both the liquid and the gas films are assumed to provide some resistance to the mass transfer. Therefore, the overall mass transfer coefficient for carbon dioxide is calculated by using equation 3-29. The equation 3-29 which is derived from two film theory, has Henry's constant

(H_{CO_2}), Enhancement factor (E) and liquid/gas mass transfer coefficient. The resistance offered by the liquid film for the mass transfer of water is considered to negligible, since the water concentration is much larger than the concentration of all other chemical compounds inside the amine solution. Therefore, the overall mass transfer coefficient for water is equal to the vapour mass transfer coefficient as shown in equation 3-28.

$$N_i = K_{G,i}(P_i - P_i^*) \quad i = H_2O, CO_2 \tag{3-27}$$

$$K_{G,H_2O} = k_{G,H_2O} \tag{3-28}$$

$$\frac{1}{K_{G,CO_2}} = \frac{RT}{k_{G,CO_2}} + \frac{H_{CO_2}}{Ek_{L,CO_2}} \tag{3-29}$$

Billet and Schultes [1999] and Onda et al. [1968] mass transfer correlations are used in the model. Billet and Schultes [1999] correlations for mass transfer coefficient can be seen in equations 3-30 and 3-31. C_l and C_g are packing dependent constants which are provided in the original paper. However, these values are not available for all the packings that are currently being used in the industry. Onda et al. [1968] correlations for mass transfer coefficients are shown in equations 3-33 and 3-32. These coefficients are functions of density, viscosity, diffusivity and packing material. If the numerical values of Onda et al. [1968] and Billet and Schultes [1999] coefficients are compared for the same case, it is noticed that the Billet and Schultes [1999] coefficient is significantly larger than the Onda et al. [1968] coefficient. The mass transfer coefficients are tested against each other for the same inlet conditions and their effects on the results can be seen in Appendix 6-7-1

$$k_L = C_l\Big(\frac{\rho_L g}{\mu_L}\Big)^{1/6}\Big(\frac{aD_L}{4\epsilon}\Big)^{1/2}\Big(\frac{u_L}{a}\Big)^{1/3} \tag{3-30}$$

$$k_G = C_g\Big(\frac{aD_G}{(4\epsilon^2 - 4\epsilon h_T)^{1/2}}\Big)\Big(\frac{\rho_G \mu_G}{a\mu_G}\Big)^{3/4}\Big(\frac{u_G}{\rho_G D_G}\Big)^{1/3} \tag{3-31}$$

$$k_G = 5.23(\frac{D_G}{ad_p})(\frac{\rho_G u_G}{a\mu_G})^{0.7}(\frac{\mu_G}{\rho_G D_G})^{1/3} \tag{3-32}$$

$$k_L = \frac{0.0051}{(ad_p)^{-0.4}}(\frac{\mu_L g}{\rho_L})^{1/3}(\frac{\rho_L u_L}{a\mu_L})^{2/3}(\frac{\mu_L}{\rho_L D_L})^{-0.5} \tag{3-33}$$

Effective interfacial area (a_w) is another important variable which is used extensively in the ODE system. Billet and Schultes [1999] and Onda et al. [1968] correlations for effective interfacial area are used with the corresponding mass transfer coefficients. The Onda et al. [1968] correlation results in a higher effective area as compared to the correlation proposed by Billet and Schultes [1999]. The effect of these correlations on the results are shown in Appendix 6-7-2.

Equations 3-34 to 3-36 are used to calculate the Enhancement factor. These correlations are proposed by Cussler [2009]. The reaction rate constant, the diffusivity of the amine in liquid solution, the concentration of the amine in the solution and the diffusivity of CO_2 in liquid solution are required to calculate the enhancement factor. While this correlation is used in this model, other correlations for enhancement factors and their effects on the results are tested in Appendix 6-7-3.

$$k_2 = 4.48x10^8 exp(\frac{-5400}{T}) \tag{3-34}$$

$$M = \frac{k_2 D_{CO_2,L} C_{MEA}}{k^2_{L,CO_2}} \tag{3-35}$$

$$E = \sqrt{M} coth(\sqrt{M}) \tag{3-36}$$

The heat transfer coefficient is calculated by using the Chilton-Colburn analogy which relates the mass transfer coefficient to the heat transfer coefficient. The exact relation is given by equation 3-38.

$$q = h(T_G - T_L) \tag{3-37}$$

$$h = k_G \left(\frac{\rho_G (c_P / M_{w,L}) \lambda^2}{D_L^2} \right)^{1/3} \tag{3-38}$$

The physical and chemical properties that are used in the model are listed in table 3-1. Accurate correlations for Enhancement factors, mass transfer coefficients, rate constants and inter-facial area are required to have accurate results.

Table 3-1: Parameters used in the Rate Based Model

Diffusivity of CO_2 in amine	Ko et al. [2001]
Diffusivity of Gas	Poling et al. [2001]
Diffusivity of Amine	Chang et al. [2005]
Surface Tension	Vazquez et al. [1997]
Heat Capacity of Gas	Poling et al. [2001]
Heat Capacity of Amine	Chiu et al. [1999]
Density of Amine	AspenTech [2013] HYSYS
Viscosity	Greer [2008]
Thermal Conductivity	Greer [2008]
Mass Transfer	Billet and Schultes [1999] and Onda et al. [1968]

3-2-2 Inlet Conditions

The model requires the composition, flow rates and temperatures of both the vapour and the liquid stream at both the ends of the absorption column. Additionally, it requires the geometry details of the absorption column and its packing.

3-2-3 Model Implementation

This type of a problem is a two point boundary value problem, there are different ways to solve it. One choice is to use an ordinary differential equation (ODE) integrator and iterate to find the accurate solution. The other choice is to use a boundary value problem (BVP) solver. For this model an open source BVP solver bvp_solver 1.1 from scikits is used. This solver requires a function which defines all the physical and chemical properties needed to calculate the derivatives of equation 3-19 to equation 3-26. It also needs a initial guess to start the solving process. The initial guess can be a profile of the variable along the length or a single value.

Chapter 4

Results and Discussions

4-1 Equilibrium Model Validation

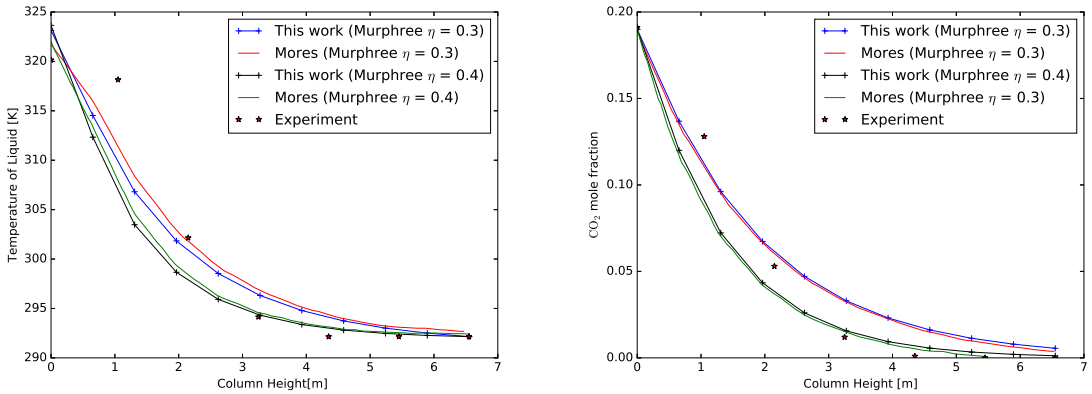

Figure 4-1: Equilibrium Model Validation. Temperature [K] vs Column Height [m] (LHS) and CO_2 mole fraction vs Column Height [m] (RHS)

Validation of the equilibrium model is done against the equilibrium model of Mores et al. [2012] to see if the model is implemented properly. The proposed equilibrium model corrects some of the errors and fills in the gaps in the model proposed by Mores et al. [2012]. The system under consideration is Run T22 of Tontiwachwuthikul et al. [1992] in which carbon dioxide is absorbed by the MEA solution in an absorption column of height 6.55m and diameter 0.1m, filled with 12.7 mm Berl Saddles packing.

Figure 4-1 shows the results of the comparison between the two equilibrium models. Both the equilibrium models are run for two different Murphree efficiencies for values of 0.3 and 0.4. The figure 4-1 shows the variation of liquid temperature (LHS) and mole fraction of carbon dioxide (RHS) in the vapour stream with the column height. The inlet conditions for the comparison are shown in the table 4-1.

Table 4-1: Inlet conditions from Tontiwachwuthikul et al. [1992]

	Flue Gas	Amine
Temperature [K]	288.15	292.15
Mole flow [mol/s]	0.14	1.03
Mole fraction of H_2O	0.10	0.94
Mole fraction of CO_2	0.19	0.0
Mole fraction of MEA	0.00	0.06
Mole fraction of N_2	0.71	0.00
Pressure [bar]	1.013	1.013

The results show that the profile of mole fraction of carbon dioxide (RHS) overlaps with the profile of Mores et al. [2012] for both the efficiencies. While the shapes of the temperature profiles (LHS) for both the efficiencies are similar, an overlap is not achieved. The reason why an exact match is not achieved for the temperature profile may be because the properties that are used for the energy equation in this work is different than the properties used by Mores et al. [2012]. The correlations used to calculate the heat capacity of the amines and gaseous stream are not disclosed in Mores et al. [2012]. These similarity in these results lead the author to deem the equilibrium model to be reliable.

4-2 Rate Based Model Validation

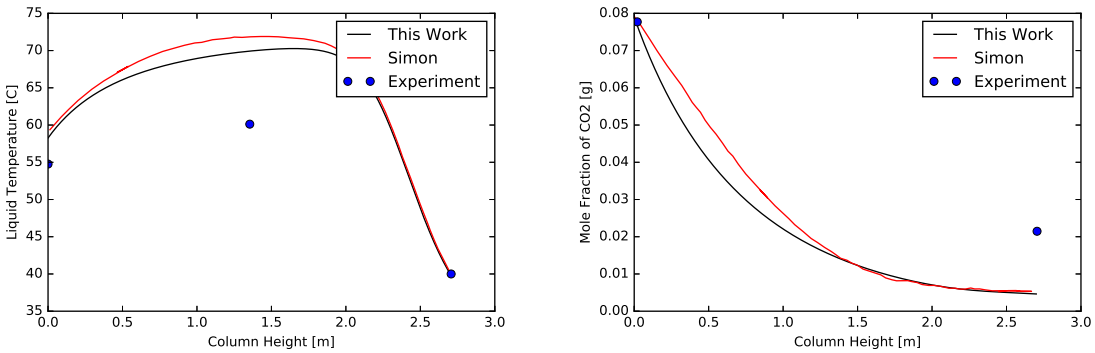

Figure 4-2: Rate Based Model Validation. Temperature [C] vs Column Height [m] (LHS) and CO_2 mole fraction vs Column Height [m] (RHS)

Validation of the rate based model is done against the rate based model of Simon et al. [2011] in order to check if the rate based model is implemented properly. Figure 4-2 shows the results of the comparison of this work and the results of the rate based model of Simon et al. [2011]. The experiment is performed on two absorption columns arranged in series which have two 1.35 m packed sections that contain 16 mm Pall rings. The amine enters the first column at a flow rate of 7 litres/ minute which uses a 30 % (w/w) of aqueous MEA as the absorbent. The flue gas enters the second column with a flow rate of 125 m^3/h with a carbon dioxide mole fraction of 0.12. The figure 4-2 shows the result of column 1.

The results show that the profiles generated by the model does not exactly match the profiles generated by the model of Simon et al. [2011] although the shapes closely resemble each other. The prediction of the outlet values of the liquid temperature and carbon dioxide mole fraction match the predictions of Simon et al. [2011]. Also, the rate based model is able to capture the temperature bulge inside the absorption column.

The difference in these profiles is attributed to the fact that the properties and parameters which are used are different in both the models. Namely, the parameters for the estimation of the mass transfer coefficients, thermal conductivity and viscosity. The reference paper did not specify the details for these properties. The model proposed by Simon et al. [2011] uses the Billet and Schultes [1999] mass transfer coefficients for water and carbon dioxide. The packing specific constants (C_l and C_g) that are used in the Billet and Schultes [1999] mass transfer coefficients for 16 mm Pall rings are not mentioned in either Billet and Schultes [1999] nor the Simon et al. [2011]. However, data was available for 50, 35 and 25 mm ceramic and metal Pall rings. The effect of these constants on the results can be seen in Appendix 6-5. The absence of this information greatly affects the results of the validation.

However, due to the similarity of all the profiles to the reference data in the absence of complete information, the author deems the rate based model to be reliable.

4-3 Model Selection

In this section, the equilibrium and rate based models are compared for four different experiments with varying conditions, in order to judge which model is able to accurately predict the experimental data.

4-3-1 Case 1: Low Flow Rate of Flue Gas

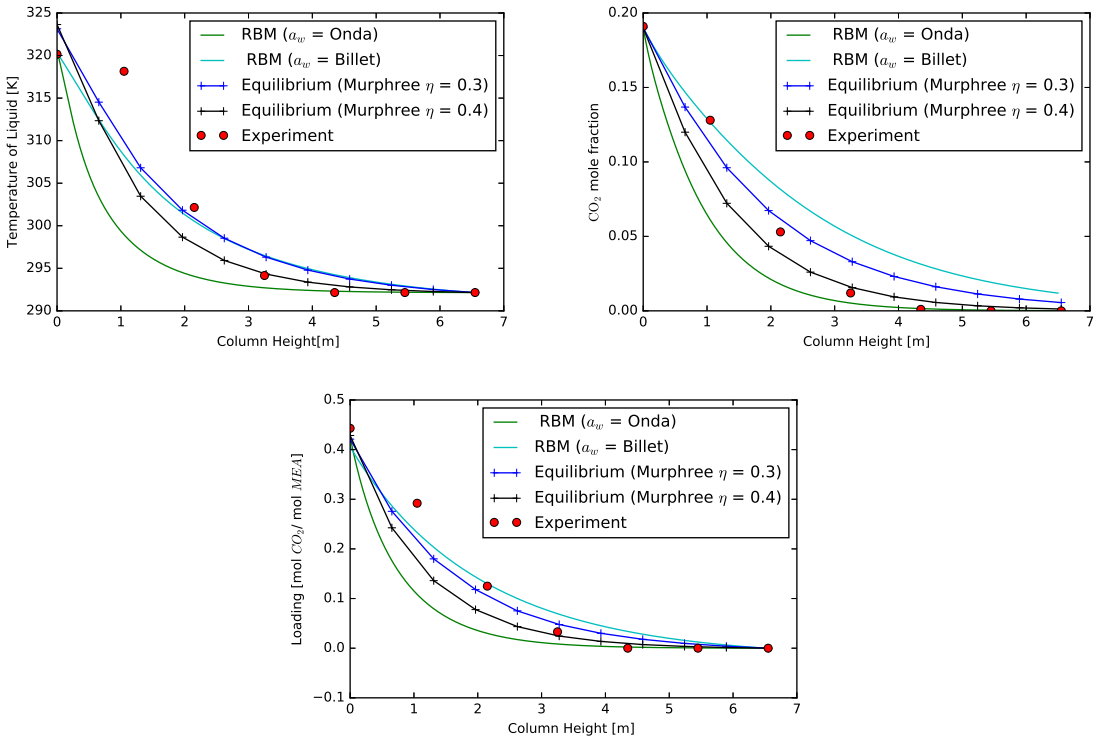

Figure 4-3: Comparison of Rate based and Equilibrium model for the experiment of Tontiwachwuthikul et al. [1992]. Temperature [K] vs Column Height [m] (LHS), CO_2 mole fraction vs Column Height [m] (RHS), Loading vs Column Height [m] (Bottom)

For the first case, the experiment of Tontiwachwuthikul et al. [1992] Run 22 is selected. This experiment was used in the validation of the equilibrium model. The results of carbon dioxide mole fraction (RHS), mole loading (Bottom) and liquid temperature (LHS) are shown in the figure 4-3. The Murphree efficiency is a parameter for the equilibrium model and it is used with the values of 0.3 and 0.4 in this comparison. The rate based model is run for two different effective area correlations, namely Onda et al. [1968] and Billet and Schultes [1999]. The results show that all four profiles do not exactly match the experimental data. However, **the equilibrium model with the efficiency of 0.4 produces the closest match to the experimental data**. The rate based model with the Onda et al. [1968] correlation of effective area has better predictions in the top portion of the column (4-6.55m). However, the slope of the profile in the bottom portion of the column (0-2m) indicates a faster rate of absorption of carbon dioxide as compared to the experimental data. The faster rate of absorption results

in a faster rate of loading of the amine which in turn affects the temperature of the liquid stream. Using effective area correlation of Billet and Schultes [1999] produces a significantly different result.

4-3-2 Case 2: Temperature Bulge with Low Flow Rate of Flue Gas

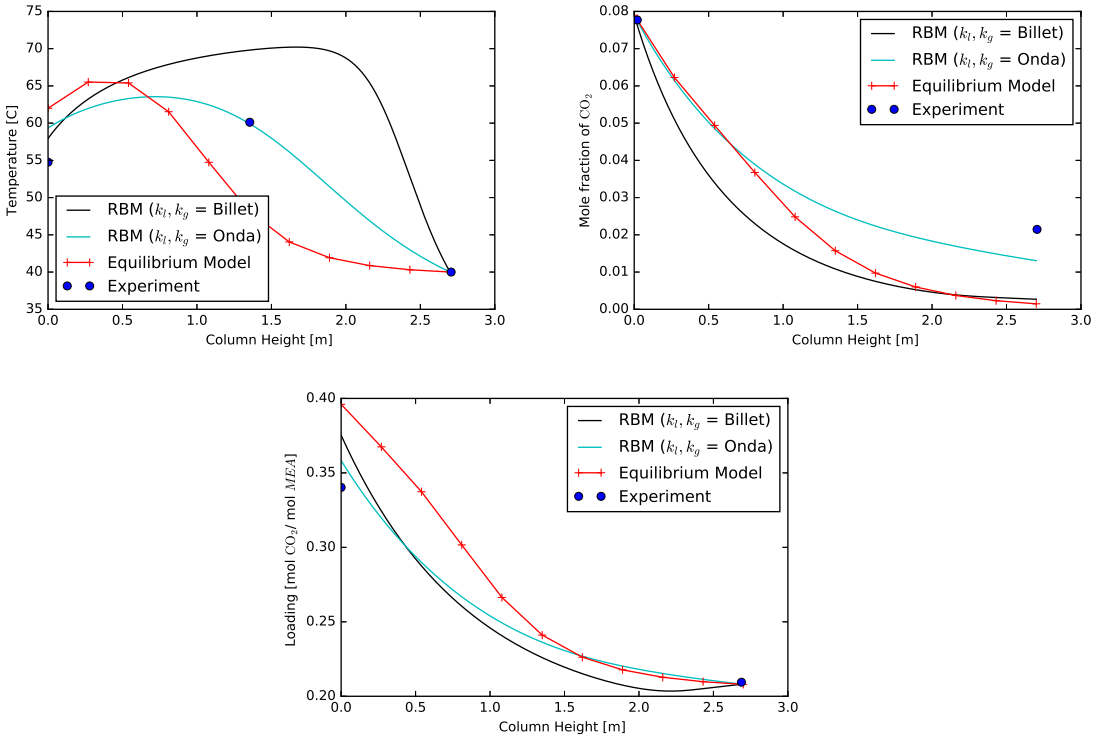

Figure 4-4: Comparison of Rate based and Equilibrium model for the experiment of Simon et al. [2011]. Temperature [K] vs Column Height [m] (LHS), CO_2 mole fraction vs Column Height [m] (RHS), Loading vs Column Height [m] (Bottom)

For the second case, the experiment of Simon et al. [2011] is selected. This case was used for the validation of the rate based model. The experimental results are only available at the inlet, outlet and the middle of the column. The results of the comparison are shown in the figure 4-4. The rate based model is run for two different correlations of mass transfer coefficients, one from Billet and Schultes [1999] and the other from Onda et al. [1968].

First, the carbon dioxide profiles (RHS) of both the models are compared against each other. The outlet values of carbon dioxide are first compared. It can be seen that the rate based model with Onda et al. [1968] correlation has the best prediction. While the predictions of the equilibrium model and rate based model with Billet and Schultes [1999] correlation are almost the same. Both these models over-predict the amount of absorption taking place in the column. Next, the mole loading profiles are compared against each other. Again, the prediction made by the rate based model with Onda et al. [1968] correlation comes closest to the experimental data of Simon et al. [2011]. The equilibrium model predicts a highest

amount of loading which differs the experimental data by approximately 17%. Since the experimental data is only available at the outlets, the profiles cannot be compared against each other. Lastly, the liquid temperature profiles are compared against each other. The experimental data indicates a presence of a temperature bulge as the temperature in the middle of the column is 61 °C, which is higher than the inlet and outlet temperatures. The results indicate that all the models predict the existence of a temperature bulge. However, it can be clearly seen that the rate based model with Onda et al. [1968] mass transfer coefficient produces the closest fit. The equilibrium model incorrectly predicts the position of the bulge. The difference between the experimental data and the equilibrium model prediction in the middle of the column is approximately 15 °C. **The rate based model clearly provides better predictions as compared to the equilibrium model.**

4-3-3 Case 3: Medium Flow Rate of Flue Gas

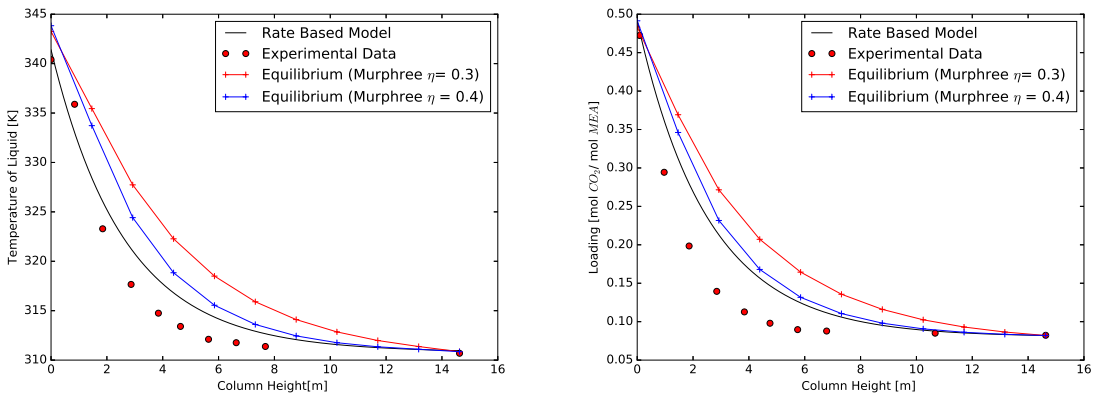

Figure 4-5: Comparison of Rate based and Equilibrium model for the experiment of Alatiqi et al. [1994]. Temperature [K] vs Column Height [m] (LHS) and Loading vs Column Height [m] (RHS)

For the third case, an independent experiment of Alatiqi et al. [1994] is selected for comparison. The input for this experiment is shown in tables 4-2 and 4-3.

Table 4-2: Inlet conditions from Alatiqi et al. [1994]

	Flue Gas	Amine
Temperature [K]	322.05	310.95
Mole flow [kmol/h]	3338.85	18984.79
Mole fraction of H_2O	0.0073	0.9261
Mole fraction of CO_2	0.1599	0.0056
Mole fraction of MEA	0.00	0.0683
Mole fraction of N_2	0.8329	0.00
Pressure [bar]	14.82	14.82

Table 4-3: Absorber Specification taken from Alatiqi et al. [1994]

Column and Packing Specifications	Values
Diameter (m)	2.74
Total packing Height	14.63
Stages	10
Packing type	Ceramic Intalox Saddles
Specific interfacial area (m^2/m^3)	625
Nominal packing size (m)	0.05
Void fraction	0.78

The results of the comparison are shown in figure 4-5. The equilibrium model is run for two efficiencies 0.3 and 0.4 and the rate based model is run by using the mass transfer coefficients of Onda et al. [1968]. The experimental values for carbon dioxide and temperature of liquid are available. The comparisons show that the rate based model gives better predictions than equilibrium model which is run at two different Murphree efficiencies. Although both the models cannot accurately predict the experimental data, the shapes of the profiles are accurately captured by both models. It must be noted that if a Murphree efficiency of 0.6 is used then a near perfect match with the experimental data. Same is true if the mass transfer coefficient of Billet and Schultes [1999] is used. However, these results shown in figures 4-6 and 4-7 respectively are not included in the comparison as the actual constants used in the mass transfer coefficients of Billet and Schultes [1999] were not found and the Murphree efficiency of 0.6 is not a commonly used value.

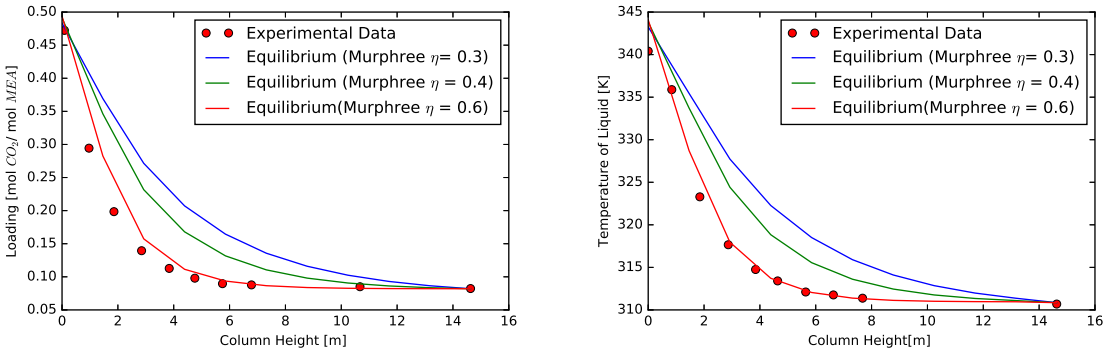

Figure 4-6: Effect of Murphree Effiency on the Equilibrium Model for the experiment of Alatiqi et al. [1994]. Temperature [K] vs Column Height [m] (LHS) and Loading vs Column Height [m] (RHS)

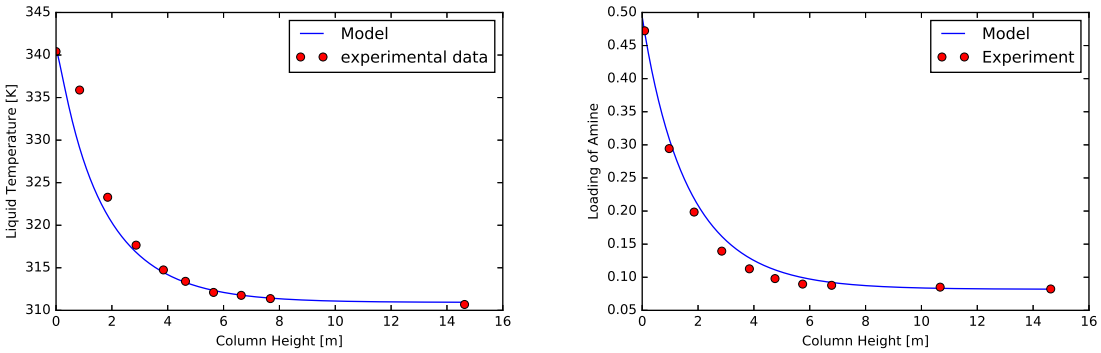

Figure 4-7: Effect of Billet and Schultes [1999] on the Rate Based Model Alatiqi et al. [1994]. Temperature [K] vs Column Height [m] (LHS) and Loading vs Column Height [m] (RHS)

4-3-4 Case 4: Temperature Bulge with Medium Flow Rate of Flue Gas

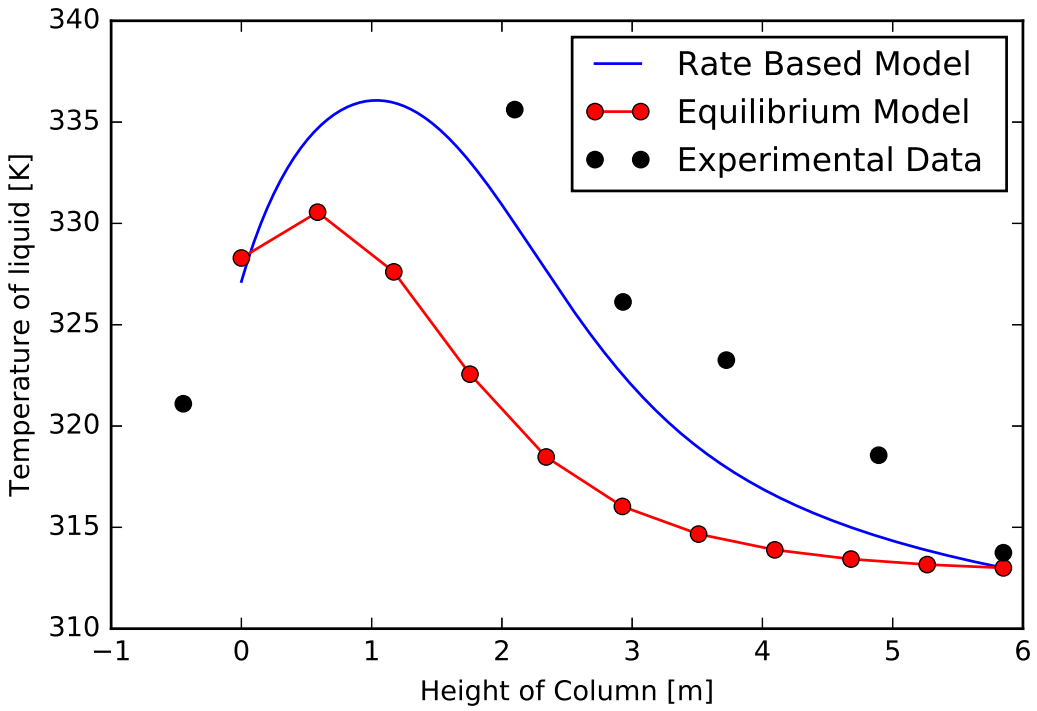

Figure 4-8: Comparison of Rate based and Equilibrium model for the experiment of Dugas [2007]. Temperature [K] vs Column Height [m]

For the final case, the experiment of Dugas [2007] was selected, whose inlet conditions and results are shown in Kvamsdal and Rochelle [2008].The inlet conditions for this case are shown in table 4-4. Only the experimental results of the temperature curve were available in Kvamsdal and Rochelle [2008]. The experimental data clearly shows a presence of a temperature

bulge. The packing height is adjusted by Kvamsdal and Rochelle [2008] to obtain the same CO_2 removal and rich loading as the pilot plant. This adjusted height of 5.85 m is used as an input instead of the actual packing height of 6.1 m. The experimental data is available at 6.1 m and not at 5.85 which can be seen in figure 4-8.

Table 4-4: Inlet conditions from Dugas [2007]

	Flue Gas	Amine
Temperature [K]	321	313
Mole flow [mol/s]	58.2	7.07
Mole fraction of H_2O	0.016	0.8756
Mole fraction of CO_2	0.165	0.0357
Mole fraction of MEA	0.00	0.1244
Mole fraction of N_2	0.819	0.00
Pressure [atm]	1	1

The results show that the temperature bulge is captured by both the models. It can be clearly seen that the liquid temperature at the outlet is almost the same for both the models. According to the experimental data, a maximum temperature of 336 K is achieved at a position of 2m from the bottom of the column. The equilibrium model predicts a maximum of 331 K at a position of 0.6 m from the bottom and the rate based model predicts a temperature of 336 K at 1.1 m from the bottom of the column. Although a perfect prediction is not made by both the models, it is clearly visible that the rate based model produces better predictions as compared to the equilibrium model.

4-4 Temperature Bulge

The next question that needed to be answered is why the temperature bulge occurs and what factors affect the position and shape of the bulge. Figure 4-9 shows the variation of mole fraction of water and vapour mole flow across the length of the column for the experiment of Dugas [2007]. It can be seen in 4-9 (LHS), that there is immediate vaporization of water on contact of the vapour stream with the amine which leads to increase in the mole fraction of water vapour from 0.01 to 0.17. The sudden vaporization causes an increase in molar flow rate of the gaseous stream from 7.1 to 8.0 mole/s.

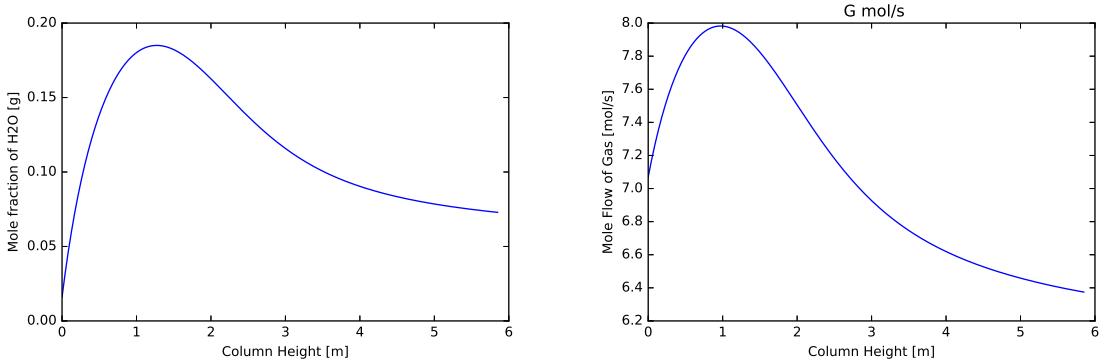

Figure 4-9: y_{H_2O} and Gas-Mole flow Profile in the experiment of Dugas [2007]

The sudden increase in water vapour mole fraction is followed by a gradual decrease which results in a bulge. The position and shape of the bulge in figure 4-9 is similar to the position and shape of the temperature bulge shown in figure 4-8. This suggests a correlation between them.

Further tests were performed to see effect of changing flow rates and compositions of the streams on the temperature profile. Figure 4-10 shows the effect of changing the Liquid to Gas mole ratio (L/G) on the temperature profile. For this test, the gas mole flow rate is varied while keeping the liquid mole flow rate to be constant. When the gas mole flow rate is increased while keeping the mole fractions to be the same, there is more amount of available water vapour and carbon dioxide which will interact with the same amount of amine solution. As the mole flow of the gas stream increases i.e. L/G decreases, the maximum temperature increases. This can be explained by the fact that more carbon dioxide is absorbed. At L/G = 8.3 i.e. normal conditions, the maximum loading of the amine at the outlet is equal to 0.40. But at L/G = 5.8, the maximum loading of amine at the outlet is equal to 0.49. Since more carbon dioxide is absorbed in the amine, there is more energy released which results in a the high temperature of 345 K. However at the same time, there is also more amount of water vapour in the inlet gaseous stream. In fact, evaporation happens till 4 m and the maximum mole fraction of water vapour achieved is 0.42. Hence, evaporation is dominant till 4m and absorption is dominant from 4-6m.

At L/G = 5.8, the bulge which was only occurring in the bottom portion of the column, is now spread out throughout the column with sharp changes at the top and bottom of the column. The reaction and evaporation takes place throughout the column which makes the bulge spread out.

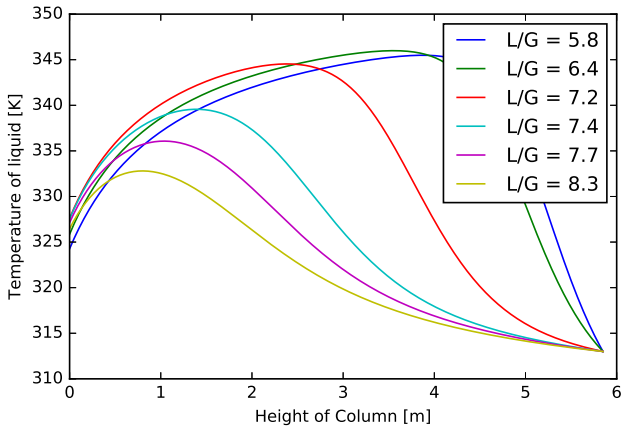

Figure 4-10: Effect of changing L/G ratio on temperature bulge in the experiment of Dugas [2007]

The effect of changing the water content in the gaseous stream was also checked on the same experiment, the results are shown in figure 4-11. It is seen that the maximum temperature increases with the increase in the water content. As the water vapour content is increased, the amount of evaporation decreases. This results in the decrease in the amount of cooling after the maxima. For $y_{H_2O} = 0.01$, there is a decrease of approximately 7K after the maxima of 333K is reached at the column height of 1.04 meters. But the decrease in temperature after the maxima for $y_{H_2O} = 0.15$ is approximately 2K. The amount of evaporation at $y_{H_2O} = 0.15$ is less than the amount of evaporation at $y_{H_2O} = 0.01$. The processes of evaporation and absorption compete against each other throughout the column. At the point of maxima, both the effects cancel each other out. In this case particular case, evaporation is dominant at the bottom of the column just before the maxima and absorption is dominant after it. As the water vapour content is increased, the opposing process to absorption decreases which results in a higher temperature and a less amount of decrease after the maxima.

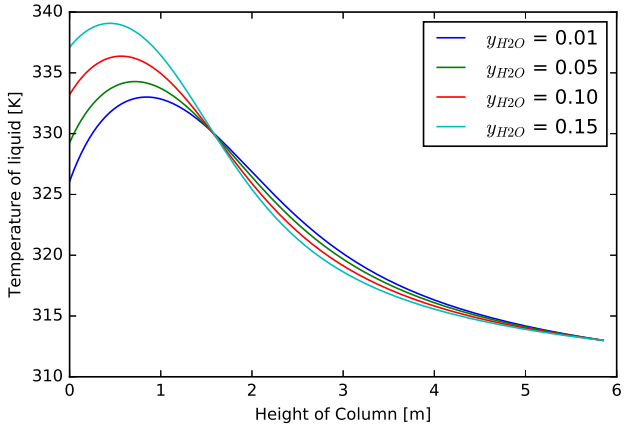

Figure 4-11: Effect of water concentration on temperature bulge

One of the interesting observations was that in the experiment of Alatiqi et al. [1994], there was no bulge seen in the temperature profile (see figure 4-5). However, the L/G ratio in that case was 5.68. This meant that L/G ratio does not solely affect the bulge and there were additional effects that were not being shown in the test. An analysis was done in order to understand exactly why that was happening. It was noticed that the water in the gaseous stream was only reaching a maximum mole fraction of 0.011 from a starting value of 0.0073 (see figure 4-12).

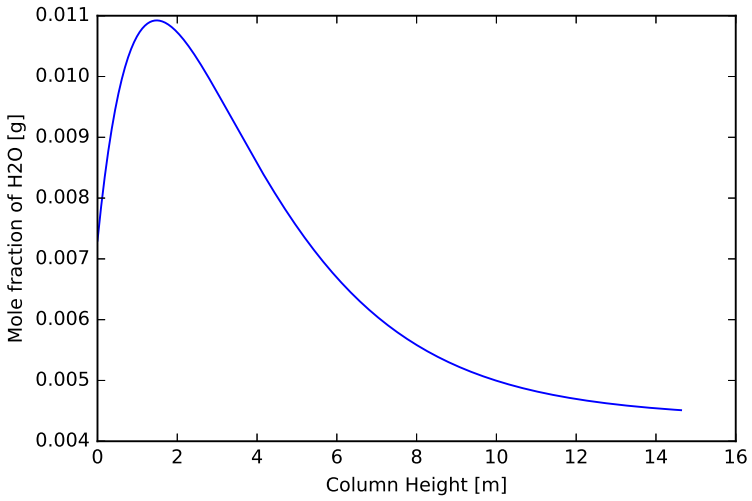

Figure 4-12: Mole fraction of H2O [g] vs Column Height [m] (LHS) at P = 14.82 bar

To check what other factors were being dominant in this experiment, inputs such as composition, temperature were altered which did not produce any significant results. Then the pressure of the column was reduced from 14.82 bar to 1 bar to see if this affected the absorption. The resulting water vapour profile and temperature profile are shown in figure 4-13. It can be clearly seen that decreasing the pressure increases the amount of evaporation of the solvent which counteracts the absorption process and produces a small bulge in the bottom of the column. The evaporation process at 14.82 bar was being dominated by the absorption process throughout the column which resulted in no bulge in the temperature profile.

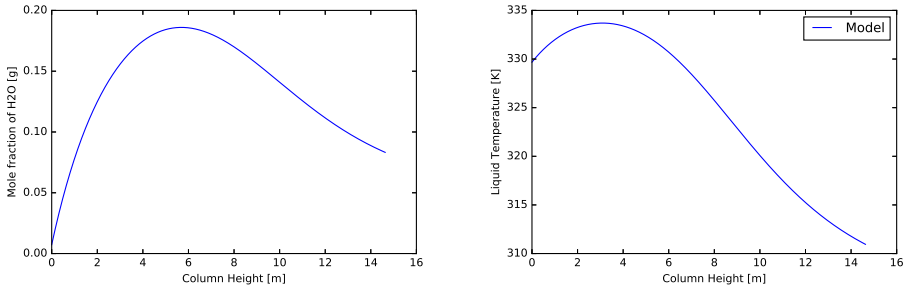

Figure 4-13: Effect of Pressure on temperature bulge in the experiment of Alatiqi et al. [1994]. Mole fraction of H2O [g] vs Column Height [m] (LHS) and Temperature of liquid stream [K] vs Column Height [m] (RHS) at P = 1 bar

Chapter 5

Conclusions and Recommendations

Two models were developed in Python^{TM} with the purpose of modelling the chemical absorption of carbon dioxide by amine in an absorption column. These two models, namely the **Equilibrium** and **Rate Based** model represent the two different approaches that exist for modelling chemical absorption. The goal of this project is to compare and determine which model can more accurately determine the experimental data and to determine the factors that affect the temperature bulge inside the absorption column. The following conclusions were drawn:

- The equilibrium and the rate based models were deemed to be reliable after validation.
- The results of the equilibrium model are dependent on the choice of the Murphree's efficiency. Currently a single value is provided by the user for the entire column. The results can be improved significantly if accurate correlations for Murphree efficiency can be used for each stage.
- The results of the rate based model are dependent on the correlations of mass transfer coefficient, effective inter-facial, rate constant and enhancement factor.
- The rate based model provides more accurate predictions of the experimental data as compared to the equilibrium model. This conclusion is drawn on the base of four tests with varying conditions. Although equilibrium model provided better predictions for one experiment, it was unable to accurately predict the position and shape of the temperature bulge.
- The temperature bulge occurs due to the opposing processes of evaporation and absorption. When the absorption process is dominating the evaporation process, there is an increase in the liquid temperature. But when evaporation of the solvent is the dominating effect, there is a decrease in temperature. The maxima is the point where both the processes cancel each other out.

- By changing the extent of evaporation relative to the extent of absorption, the position and shape of temperature bulge can be altered. This can be achieved by changing the L/G ratio, water vapour content and changing the total pressure of the system among other options.
- The author faced difficulty translating models presented in papers into working models as the entire information was not disclosed.

5-1 Future work

Firstly, both the models can be easily adapted for any amine by changing the properties such as viscosity, conductivity etc. While this work is centered around the use of MEA, different amines can be used if the neccessary physcial properties and kinetic models are obtained.

The model is recommended to be used to model the HIDIC Column. In order to do this, the distributions of both the vapour and liquid streams into different channels must be modelled which will be added to the existing rate based model.

Another interesting aspect of the rate based model is its dependency on the correlations of mass transfer coefficient, enhancement factor, rate constant. While a small study is shown in this work in the Appendix, an extensive study could be conducted to test all the combinations. The aim of this study could be to establish which sets of correlations are best suited for different conditions.

Chapter 6

Appendix

6-1 Henry's Law

The Henry's law constant for CO_2 in MEA solution is obtained by using the N_2O analogy. where $H_{N_2O,MEA}$ refers to Henry's constant of N_2O in MEA, and $H_{N_2O,water}$, $H_{CO_2,water}$ refer to the Henry's constant of N_2O and CO_2 in water whose values were taken from Versteeg and Van Swaaij [1988]

$$H_{CO_2,water} = 2.82x10^{6}exp(\frac{-2044}{T_L}) \tag{6-1}$$

$$H_{N_2O,water} = 8.55x10^{6}exp(\frac{-2284}{T_L}) \tag{6-2}$$

$$H_{N_2O,MEA} = d_1exp(\frac{d_2}{T_L}) \tag{6-3}$$

where d_1 and d_2 are taken from Wang et al. [1992].

$$a_{ij} = 4.793 - 7.446x10^{-3} * T - 2.201\phi_{MEA} \tag{6-4}$$

$$ln(He) = \phi_{MEA}\phi_{H_2O}a_{ij} + \phi_{MEA}ln(He_{N_2O,MEA}) + \phi_{H_2O}ln(He_{N_2O,H_2O}) \tag{6-5}$$

6-2 Equilibrium Constant

The equilibrium constants used in the equilibrium model for monoethanolamine are displayed in table 6-1 for the constants mentioned in equations 3-1 to 3-5. These constants are taken from Aboudheir et al. [2003].

Table 6-1: Equilibrium constant lnK = a1/T + a2lnT + a3 mentioned in equations 3-1 to 3-5

	a1	a2	a3	T range [K]
K1	140.932	-13445.9	-22.4773	273-498
K2	235.482	-12,092	-36.7816	273-498
K3	220.067	-12431.7	-35.4819	273-498
K4	6.69425	-3090.83	0	298-413
K5	-3.3636	-5851.11	0	0

6-3 Antoine Coefficient

Antoine coefficients for water are shown in in table 6-2. These constants are used in equation 6-6.

Table 6-2: Antoine's Constant for water

-	A	B	C
P_{H_2O}	5.20389	1733.926	-39.485

$$\log_{10}\mathrm{P} = \mathrm{A} - (\mathrm{B}/(\mathrm{T} + \mathrm{C})) \tag{6-6}$$

6-4 Molecular Weight

The molar weights which were used in the equilibrium model to perform the mass balance checks are shown in table 6-3.

Table 6-3: Molecular Weight of chemical species involved in modelling

CO_2	MEA	H_2O	N_2	O_2	$MEAH^+$	$MEACOO^-$	HCO_3^-	CO_3^{2-}	OH^-	H_3O^+
44	61	18	28	32	62	104	61	60	17	19

6-5 Effect of Billet Coefficients on Rate-Based Model

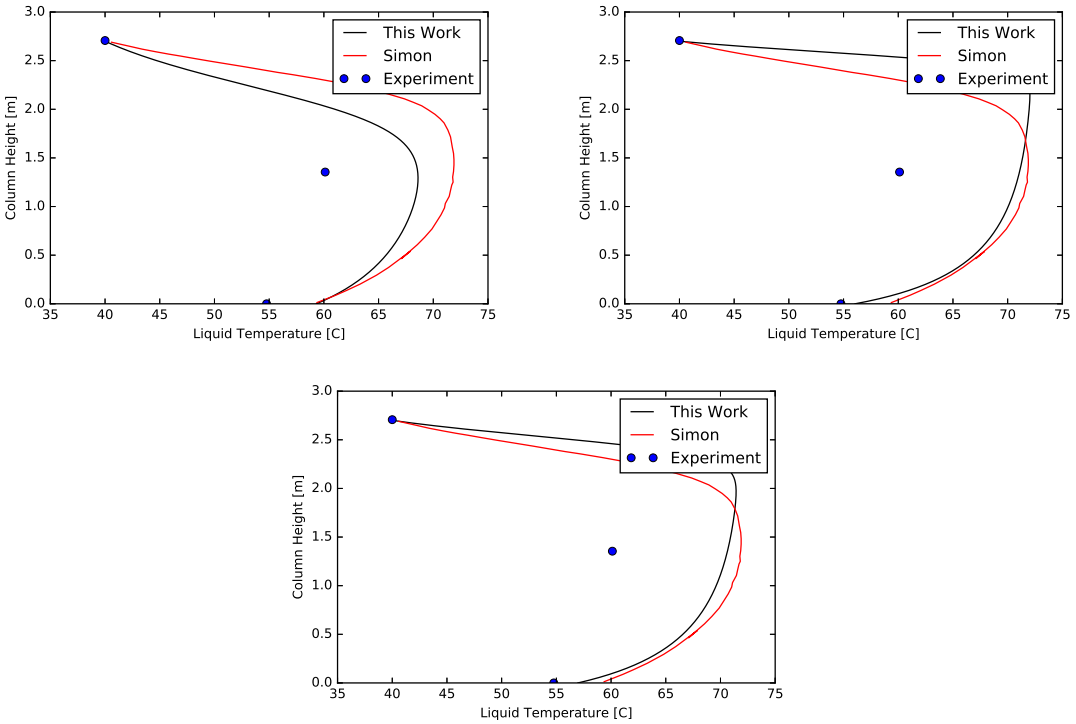

Figure 6-1: Effect of Billet and Schultes [1999] constants on the results of Rate-Based model. $C_l = 0.3$(LHS), $C_l = 0.6$ (RHS) and $C_l = 0.8$ (Bottom)

The constant C_l and C_g which are used in equation 6-7 and equation 6-8 are dependent on the type of packing used. These values were unavailable for the experiment of Simon et al. [2011]. The effect of changing these values can be seen in figure 6-1.

$$k_L = C_l\left(\frac{\rho_L g}{\mu_L}\right)^{1/6}\left(\frac{aD_L}{4\epsilon}\right)^{1/2}\left(\frac{u_L}{a}\right)^{1/3} \tag{6-7}$$

$$k_G = C_g\left(\frac{aD_G}{(4\epsilon^2 - 4\epsilon h_T)^{1/2}}\right)\left(\frac{\rho_G \mu_G}{a\mu_G}\right)^{3/4}\left(\frac{u_G}{\rho_G D_G}\right)^{1/3} \tag{6-8}$$

Several combinations between these constants are possible which would significantly alter the results. This is the disadvantage of using Billet and Schultes [1999] mass transfer coefficient for new packings.

6-6 Chemical Kinetics Model for Equilibrium-Stage Model

The equilibrium model is based on the chemical model that captures the kinetics of the carbon dioxide absorption in monoethanolamine which is proposed by Aboudheir et al. [2003]. Figure 6-2 shows the change in concentrations of the chemical ions with change in loading. The

replication of the kinetics is essential in the building of the equilibrium model. The figure 6-2 proves that the kinetics of the carbon dioxide absorption are accurately depicted. The A in the legend of figure 6-2 refers to the article of Aboudheir et al. [2003] and M refers to the model.

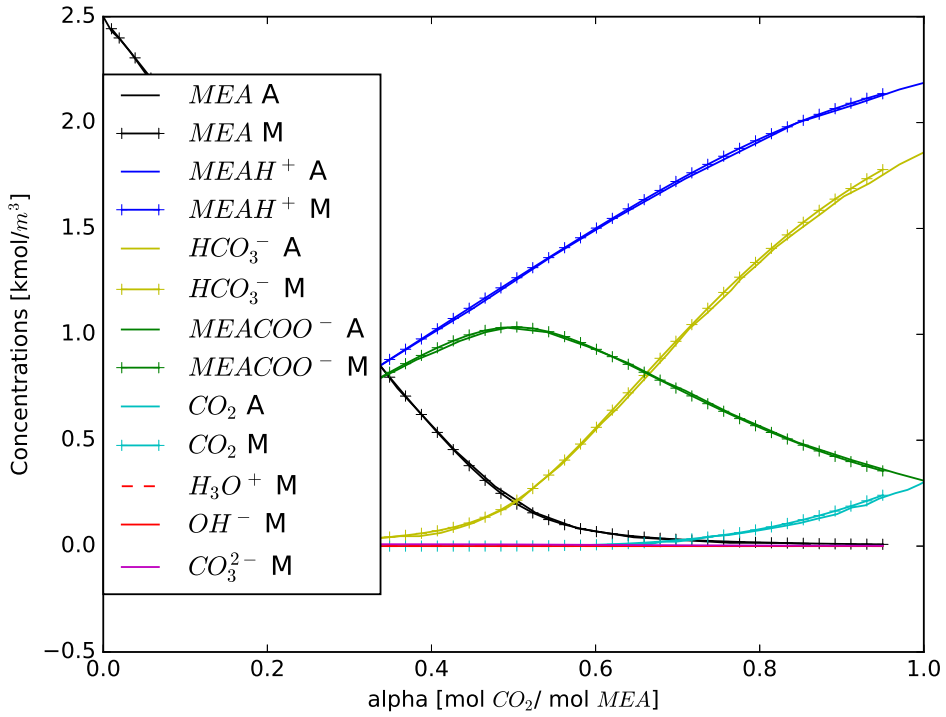

Figure 6-2: Comparison of Aboudheir et al. [2003] and Model predictions of concentrations

The equilibrium partial pressures of carbon dioxide in the model and Aboudheir et al. [2003] do not overlap perfectly as shown in figure 6-3 . According to Aboudheir et al. [2003], the typical range of uncertainty in vapour liquid equilibrium data for carbon dioxide - monoethanol amine system is 20%. In order to get a perfect match, the Henry's constant is altered so as to match the data from Aboudheir et al. [2003].

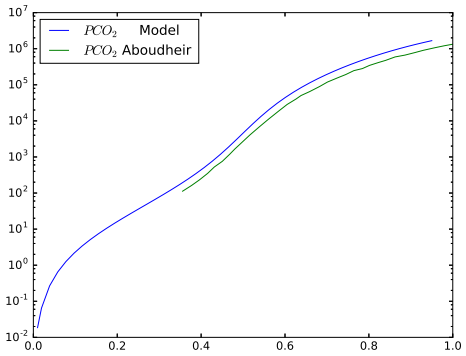

Figure 6-3: Comparison of equilibrium partial pressure of CO_2

6-7 Effect of Correlations on Rate Based Model

While customizing the model for amine solvent, it was noticed that using different correlation produced significantly different results.So different correlations for mass transfer coefficient, effective area, enhancement factor and rate constant were tested for the experiment of Tontiwachwuthikul et al. [1992] to see if there would be any change in the results. In this section, the results of those tests are presented. The properties that are used in the rate based model which is used as the base model are described in table 3-1. For this comparison, the correlations of Enhancement factor, rate constant, mass transfer coefficient and effective area of mass transfer are substituted while keeping the other properties constant. The results of this test is shown in this section.

6-7-1 Effect of Mass Transfer coefficient on the Rate Based Model

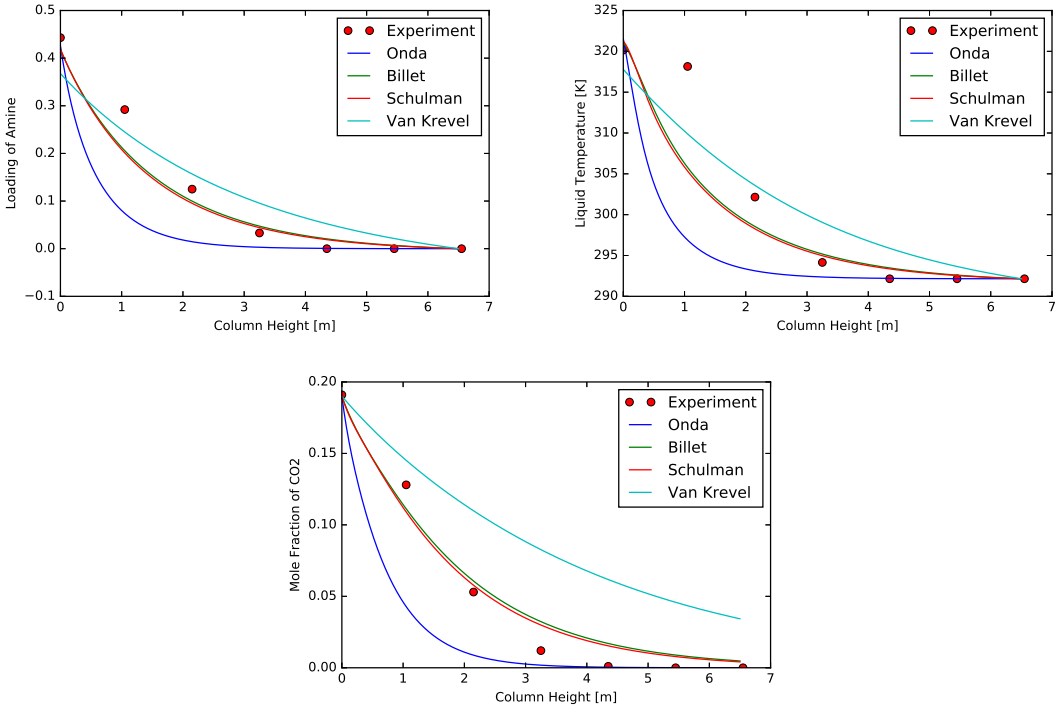

Figure 6-4: Effect of Mass transfer coefficients

In the first test, different correlations for the mass transfer coefficient were tested in the program. The different relations used and their sources are mentioned in table 6-4. It can be seen that the choice of mass transfer coefficient used greatly affects the results of the model. While the original model used the mass transfer coefficient of Billet and Schultes [1999]. The coefficient taken from Shulman et al. [1955] is also able to follow the profile quite reasonably. Whereas the correlations from Onda et al. [1968] and van Krevelen and Hoftijzer [1948] do not give accurate results.

Table 6-4: Mass Transfer Coefficients

Source	Equation
Billet and Schultes [1999]	$k_L = 1.364\left(\frac{\rho_L g}{\mu_L}\right)^{1/6}\left(\frac{aD_L}{4\epsilon}\right)^{1/2}\left(\frac{u_L}{a}\right)^{1/3}$
	$k_G = 0.232\left(\frac{aD_G}{(4\epsilon^2 - 4\epsilon h_T)^{1/2}}\right)\left(\frac{\rho_G \mu_G}{a\mu_G}\right)^{3/4}\left(\frac{u_G}{\rho_G D_G}\right)^{1/3}$
Onda et al. [1968]	$k_G = 5.23(\frac{D_G}{ad_p})(\frac{\rho_G u_G}{a\mu_G})^{0.7}(\frac{\mu_G}{\rho_G D_G})^{1/3}$
	$k_L = \frac{0.0051}{(ad_p)^{-0.4}}(\frac{\mu_L g}{\rho_L})^{1/3}(\frac{\rho_L u_L}{a\mu_L})^{2/3}(\frac{\mu_L}{\rho_L D_L})^{-0.5}$
	$d_p =$ Particle diameter
Shulman et al. [1955]	$k_G = 1.195 u_G[\frac{d_p \rho_G u_G}{\mu_G(1-\epsilon)}]^{-0.36} Sc_G^{-2/3}$
	$k_L = 25.1\frac{D_L}{d_p}(\frac{d_p \rho_L u_L}{\mu_L})^{0.45} Sc_L^{0.5}$
van Krevelen and Hoftijzer [1948]	$k_G = 0.2\frac{D_G}{d_c}(\frac{\rho_L u_L}{a\mu_L})^{0.8} Sc_G^{1/3}$
	$k_L = 0.015\frac{D_L}{[\mu_L/(\rho_L^2 g)]^{1/3}}(\frac{\rho_L u_L}{a\mu_L})^{2/3} Sc_L^{1/3}$

6-7-2 Effect of Effective Inter-facial Area on the Rate Based Model

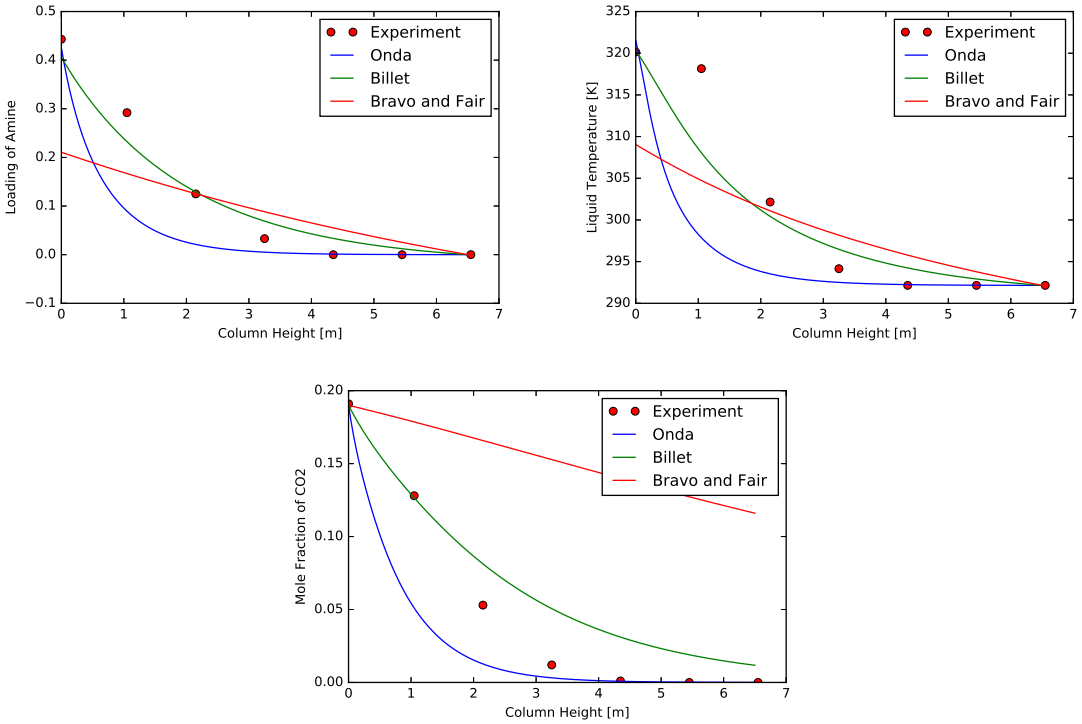

Figure 6-5: Effect of effective area correlation

In the second test, 3 different correlations for the effective inter-facial area are tested. The correlations are shown in table 6-5. From the results shown in figure 6-5, it can be seen that the correlation of Billet and Schultes [1999] and Onda et al. [1968] produce the closest match with the experimental data.

Table 6-5: Effective Interfacial Area correlations for the rate based model

Source	Equation
Billet and Schultes [1999]	$a_w = 1.5a(ad_h)^{-0.5}(\frac{u_L d_h}{\nu_L})^{-0.2}(\frac{u_L^2 \rho_L d_h}{\sigma_L})^{0.75}(\frac{u_L^2}{g d_h})^{-0.45}$
Onda et al. [1968]	$a_w = a(1 - \exp(-1.45(\frac{\sigma_C}{\sigma_L})Re_L^{0.1}Fr_L^{-0.05}We_L^{0.2}))$
Bravo and Fair [1982]	$0.498(\frac{u_L \mu_L}{\sigma_L}\frac{6\rho_G u_G}{a\mu_G})^{0.392}\frac{\sigma_L^{0.5}}{Height^{0.4}}$

6-7-3 Effect of Enhancement Factor on the Rate-Based Model

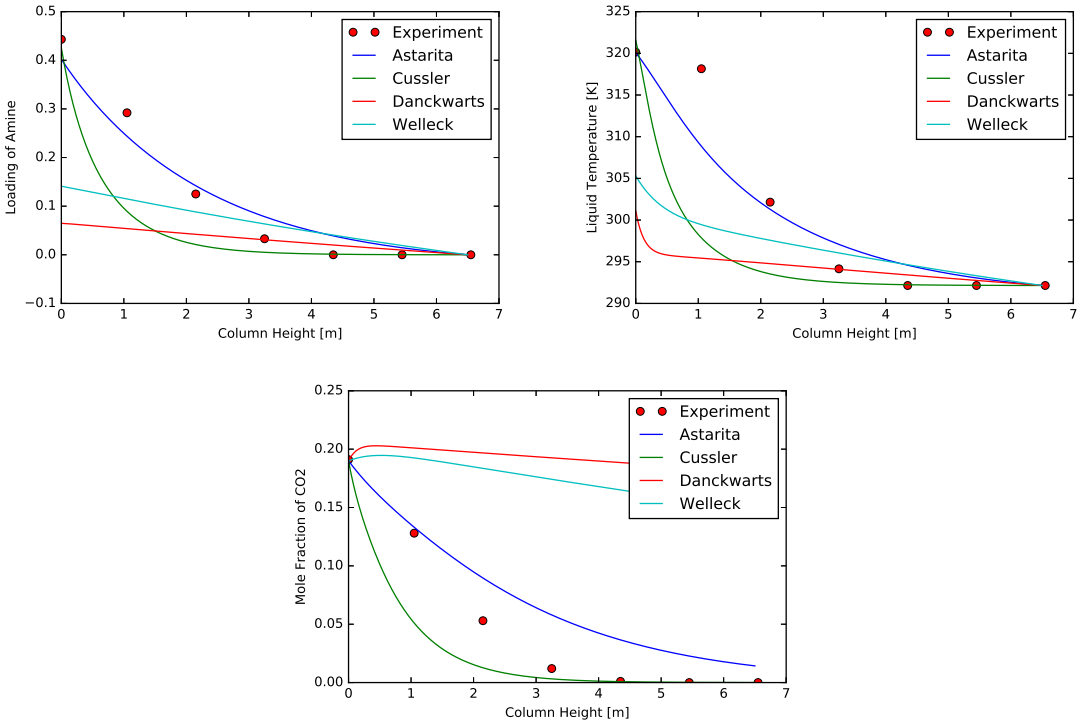

Figure 6-6: Effect of Enhancement factor on results of Rate-Based model for Tontiwachwuthikul et al. [1992]

In the third test, different correlations for Enhancement factors were tested which are shown in table 6-6. It can be seen from the results that the Cussler [2009] correlation and Astarita correlation from van Krevelen and Hoftijzer [1948] give the best predictions. Wellek et al. [1978] underestimates the absorption of CO_2 by a considerable margin whereas the correlation from Danckwerts [1955] massively underestimates the absorption.

Table 6-6: Enhancement factor

Source	Equation
Danckwerts [1955]	$E = \sqrt{1 + \frac{D_{CO_2,L} k_2}{k_L^2}}$
Astarita from van Krevelen and Hoftijzer [1948]	$E = [(1 + \frac{n^{n/n-1}(E_\infty - 1)^{1/(n-1)} E_\infty}{(1+M)^{n/(2n-2)}}) - 1]^1$ $\frac{(1+M)^{n/(2n-2)}}{n^{1/(n-1)}(E_\infty - 1)^{1/(n-1)}}$
Cussler from Wellek et al. [1978]	$E = \sqrt{M}\coth(\sqrt{M})$
Wellek et al. [1978] used in Afkhamipour and Mofarahi [2013]	$E = 1 + \frac{1}{[(1/(E_\infty - 1))^{1.35} + (1/(E_1 - 1))^1.}$

6-7-4 Effect of Rate Constant on the Rate Based Model

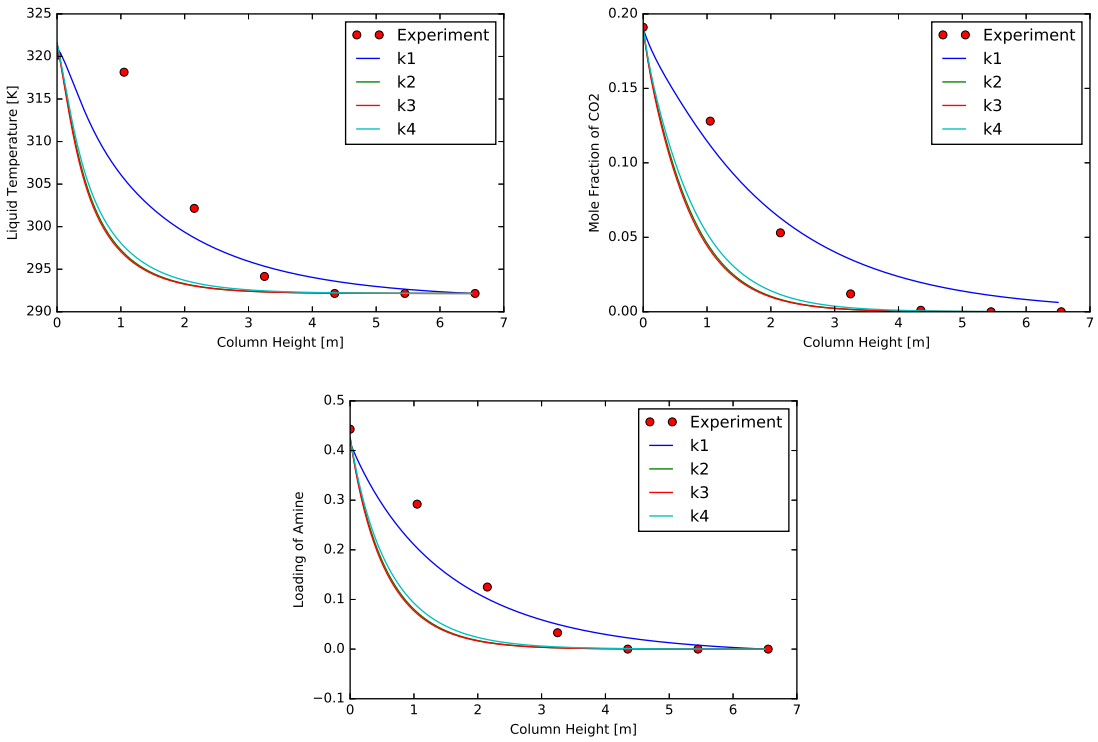

Figure 6-7: Effect of Rate constants on results of Rate-Based model for Tontiwachwuthikul et al. [1992]

In the fourth and final test, different correlations for rate constants are tested which are listed in 6-7. It can be seen that three of the four relations produce identical results. However, the relation from Aboudheir et al. [2003] produces a slightly different result which appears to produce a better match than the other three.

Table 6-7: Rate Constants

Source	Equation
Aboudheir et al. [2003]	$k_1 = 4.61x10^9 exp(\frac{-4412}{T})$
Versteeg and Van Swaaij [1988]	$k_2 = 4.48x10^8 exp(\frac{-5400}{T})$
Horng and Li [2002]	$k_3 = 3.01x10^8 exp(\frac{-5376}{T})$
Hikita et al. [1977]	$k_4 = 9.77x10^7 exp(\frac{-4955}{T})$

Bibliography

A. Aboudheir, P. Tontiwachwuthikul, A. Chakma, and R. Idem. Kinetics of the reactive absorption of carbon dioxide in high CO_2 loaded, concentrated aqueous monoethanolamine solutions. *Chemical Engineering Science*, 58(23-24):5195 – 5210, 2003. ISSN 0009-2509. doi: http://dx.doi.org/10.1016/j.ces.2003.08.014. URL http://www.sciencedirect.com/science/article/pii/S0009250903004196.

M. Afkhamipour and M. Mofarahi. Comparison of rate-based and equilibrium-stage models of a packed column for post-combustion {CO2} capture using 2-amino-2-methyl-1-propanol (amp) solution. *International Journal of Greenhouse Gas Control*, 15:186 – 199, 2013. ISSN 1750-5836. doi: http://dx.doi.org/10.1016/j.ijggc.2013.02.022. URL http://www.sciencedirect.com/science/article/pii/S1750583613001163.

N.A. Al-Baghli, S.A. Pruess, V.F. Yesavage, and Selim M.S. A rate based model for the design of gas absorbers for the removal of CO_2 and H_2S using aqueous solutions of mea and dea. *Fluid Phase Equilibria*, 185(1-2):31–43, 2001. ISSN 0378-3812. doi: http://dx.doi.org/10.1016/S0378-3812(01)00454-X. URL http://www.sciencedirect.com/science/article/pii/S037838120100454X. Proceedings of the 14th symposium on thermophysical properties.

I. Alatiqi, M.F. Sabri, W. Bouhamra, and E. Alper. Steady-state rate-based modelling for CO_2/amine absorption and desorption systems. *Gas Separation and Purification*, 8(1):3–11, 1994. ISSN 0950-4214. doi: http://dx.doi.org/10.1016/0950-4214(94)85002-X. URL http://www.sciencedirect.com/science/article/pii/095042149485002X.

AspenTech. Aspen hysys, 2013.

R. Billet and M. Schultes. Prediction of mass transfer columns with dumped and arranged packings. *Chemical Engineering Research and Design*, 77(6):498 – 504, 1999. ISSN 0263 - 8762. doi: http://dx.doi.org/10.1205/026387699526520. URL http://www.sciencedirect.com/science/article/pii/S0263876299718186.

J. L. Bravo and J. R. Fair. Generalized correlation for mass transfer in packed distillation columns. *Industrial and Engineering Chemistry Process Design and Development*,

21(1):162–170, 1982. doi: 10.1021/i200016a028. URL http://dx.doi.org/10.1021/i200016a028.

L.C. Chang, T.I. Lin, and M.H. Li. Mutual diffusion coefficients of some aqueous alkanolamines solutions. *Journal of Chemical and Engineering Data*, 50(1):77–84, 2005. doi: 10.1021/je049828h. URL http://dx.doi.org/10.1021/je049828h.

L.F. Chiu, H.F. Liu, and M.H. Li. Heat capacity of alkanolamines by differential scanning calorimetry. *Journal of Chemical and Engineering Data*, 44(3):631–636, 1999. doi: 10.1021/je980217x. URL http://dx.doi.org/10.1021/je980217x.

E.L. Cussler. *Diffusion-Mass transfer in fluid systems*. Cambridge University Press, 2009.

P. V. Danckwerts. Gas absorption accompanied by chemical reaction. *AIChE Journal*, 1(4):456–463, 1955. ISSN 1547-5905. doi: 10.1002/aic.690010412. URL http://dx.doi.org/10.1002/aic.690010412.

R.E Dugas. *Pilot plant study of Carbon Dioxide capture by Aq. Monoethanolamine*. Phd thesis, University of Texas at Austin, 2007.

EngineeringToolbox.com. Fluids - latent heat of evaporation, 2016. URL http://www.engineeringtoolbox.com/fluids-evaporation-latent-heat-d_147.html.

Microsoft Excel. Microsoft excel, 2013.

L. Faramarzi, G.M. Kontogeorgis, M. L. Michelsen, K. Thomsen, and E.H. Erling H. Stenby. Absorber model for CO_2 capture by monoethanolamine. *Industrial and Engineering Chemistry Research*, 49(8):3751–3759, 2010. doi: 10.1021/ie901671f. URL http://dx.doi.org/10.1021/ie901671f.

J. Gabrielsen, M. L. Michelsen, E. H. Stenby, and G. M. Kontogeorgis. Modeling of CO_2 absorber using an amp solution. *AIChE Journal*, 52(10):3443–3451, 2006. ISSN 1547-5905. doi: 10.1002/aic.10963. URL http://dx.doi.org/10.1002/aic.10963.

T. Greer. Modeling and simulation of post combustion CO_2 capturing. Master thesis, Telemark University College, 2008.

H. Hikita, S. Asai, H. Ishikawa, and M. Honda. The kinetics of reactions of carbon dioxide with monoethanolamine, diethanolamine and triethanolamine by a rapid mixing method. *The Chemical Engineering Journal*, 13(1):7 – 12, 1977. ISSN 0300-9467. doi: http://dx.doi.org/10.1016/0300-9467(77)80002-6. URL http://www.sciencedirect.com/science/article/pii/0300946777800026.

K.A. Hoff. *Modeling and Experimental Study of Carbon Dioxide Absorption in A Membrane Contactor*. Phd thesis, Norwegian University of Science and Technology, 2003.

S.Y. Horng and M.H. Li. Kinetics of absorption of carbon dioxide into aqueous solutions of monoethanolamine + triethanolamine. *Industrial and Engineering Chemistry Research*, 41(2):257–266, 2002. doi: 10.1021/ie010671l. URL http://dx.doi.org/10.1021/ie010671l.

F.M. Khan, V. Krishnamoorthi, and T. Mahmud. Modelling reactive absorption of CO_2 in packed columns for post-combustion carbon capture applications. *Chemical Engineering Research and Design*, 89(9):1600 – 1608, 2011. ISSN 0263-8762. doi: http://dx.doi.org/10.1016/j.cherd.2010.09.020. URL http://www.sciencedirect.com/science/article/pii/S026387621000287X. Special Issue on Carbon Capture amp Storage.

J.J. Ko, T.C. Tsai, C.Y. Lin, H.M. Wang, and M.H. Li. Diffusivity of nitrous oxide in aqueous alkanolamine solutions. *Journal of Chemical and Engineering Data*, 46(1):160–165, 2001. doi: 10.1021/je000138x. URL http://dx.doi.org/10.1021/je000138x.

L. Kucka, I. Muller, E.Y. Kenig, and A. Gorak. On the modelling and simulation of sour gas absorption by aqueous amine solutions. *Chemical Engineering Science*, 58(16):3571 – 3578, 2003. ISSN 0009-2509. doi: http://dx.doi.org/10.1016/S0009-2509(03)00255-0. URL http://www.sciencedirect.com/science/article/pii/S0009250903002550.

H. M. Kvamsdal and G. T. Rochelle. Effects of the temperature bulge in CO_2 absorption from flue gas by aqueous monoethanolamine. *Industrial & Engineering Chemistry Research*, 47(3):867–875, 2008. doi: 10.1021/ie061651s. URL http://dx.doi.org/10.1021/ie061651s.

H.M. Kvamsdal, J.P. Jakobsen, and K.A. Hoff. Dynamic modeling and simulation of a CO_2 absorber column for post-combustion CO_2 capture. *Chemical Engineering and Processing: Process Intensification*, 48(1):135 – 144, 2009. ISSN 0255-2701. doi: http://dx.doi.org/10.1016/j.cep.2008.03.002. URL http://www.sciencedirect.com/science/article/pii/S0255270108000718.

Metoffice.gov.uk. Met office hadley centre observations datasets, 2016. URL http://www.metoffice.gov.uk/hadobs/hadcrut4/data/current/download.html.

M. Mofarahi, Y. Khojasteh, H. Khaledi, and A. Farahnak. Design of CO_2 absorption plant for recovery of CO_2 from flue gases of gas turbine. *Energy*, 33(8):1311 – 1319, 2008. ISSN 0360-5442. doi: http://dx.doi.org/10.1016/j.energy.2008.02.013. URL http://www.sciencedirect.com/science/article/pii/S0360544208000637.

P. Mores, N. Scenna, and S. Mussati. A rate based model of a packed column for CO_2 absorption using aqueous monoethanolamine solution. *International Journal of Greenhouse Gas Control*, 6:21 – 36, 2012. ISSN 1750-5836. doi: http://dx.doi.org/10.1016/j.ijggc.2011.10.012. URL http://www.sciencedirect.com/science/article/pii/S1750583611002040.

K. Onda, H. Takeuchi, and Y. Okumoto. Mass transfer coefficients between gas and liquid phases in packed columns. *Journal of Chemical Engineering of Japan*, 1(1):56 – 62, 1968.

J.D. Pandya. Adiabatic gas absorption and stripping with chemical reaction in packed towers. *Chemical Engineering Communications*, 19(4-6):343–361, 1983. doi: 10.1080/00986448308956351. URL http://dx.doi.org/10.1080/00986448308956351.

B.E. Poling, J.M. Prausnitz, and J. P. O'Connell. *The properties of Gases and Liquids*. McGraw-Hill, fifth edition edition, 2001. ISBN 9780070116825.

Separation Process. Murphree efficiency, 2016. URL http://www.separationprocesses.com/Distillation/DT_Chp04p2.htm.

Separation Processes. Absorption, 2016. URL http://www.separationprocesses.com.

H. L. Shulman, C. F. Ullrich, A. Z. Proulx, and J. O. Zimmerman. Performance of packed columns. ii. wetted and effective-interfacial areas, gas and liquid-phase mass transfer rates. *AIChE Journal*, 1(2):253–258, 1955. ISSN 1547-5905. doi: 10.1002/aic.690010220. URL http://dx.doi.org/10.1002/aic.690010220.

L.L. Simon, Y. Elias, G. Puxty, Y. Artanto, and K. Hungerbuhler. Rate based modeling and validation of a carbon-dioxide pilot plant absorbtion column operating on monoethanolamine. *Chemical Engineering Research and Design*, 89(9):1684 – 1692, 2011. ISSN 0263-8762. doi: http://dx.doi.org/10.1016/j.cherd.2010.10.024. URL http://www.sciencedirect.com/science/article/pii/S0263876210003266. Special Issue on Carbon Capture and amp Storage.

R. Taylor and Krishna. *Multicomponent Mass Transfer*. Wiey, 1993. ISBN 978-0-471-57417-0. URL http://eu.wiley.com/WileyCDA/WileyTitle/productCd-0471574171.html.

P. Tontiwachwuthikul, A. Meisen, and C.J. Lim. CO_2 absorption by naoh, monoethanolamine and 2-amino-2-methyl-1-propanol solutions in a packed column. *Chemical Engineering Science*, 47(2):381 – 390, 1992. ISSN 0009-2509. doi: http://dx.doi.org/10.1016/0009-2509(92)80028-B. URL http://www.sciencedirect.com/science/article/pii/000925099280028B.

D. W. van Krevelen and P. J. Hoftijzer. Kinetics of gas-liquid reactions part i. general theory. *Recueil des Travaux Chimiques des Pays-Bas*, 67(7):563–586, 1948. ISSN 0165-0513. doi: 10.1002/recl.19480670708. URL http://dx.doi.org/10.1002/recl.19480670708.

G. Vazquez, E. Alvarez, J. M. Navaza, R. Rendo, and E. Romero. Surface tension of binary mixtures of water + monoethanolamine and water + 2-amino-2-methyl-1-propanol and tertiary mixtures of these amines with water from 25 c to 50 c. *Journal of Chemical and Engineering Data*, 42(1):57–59, 1997. doi: 10.1021/je960238w. URL http://dx.doi.org/10.1021/je960238w.

G. F. Versteeg and W. Van Swaaij. Solubility and diffusivity of acid gases (carbon dioxide, nitrous oxide) in aqueous alkanolamine solutions. *Journal of Chemical & Engineering Data*, 33(1):29–34, 1988. doi: 10.1021/je00051a011. URL http://dx.doi.org/10.1021/je00051a011.

G. Q. Wang, X. G. Yuan, and K. T. Yu. Review of mass-transfer correlations for packed columns. *Industrial & Engineering Chemistry Rxesearch*, 44(23):8715–8729, 2005. doi: 10.1021/ie050017w. URL http://dx.doi.org/10.1021/ie050017w.

Y.W. Wang, S. Xu, F.D. Otto, and A.E. Mather. Solubility of N_2O in alkanolamines and in mixed solvents. *The Chemical Engineering Journal*, 48(1):31 – 40, 1992. ISSN 0300-9467. doi: http://dx.doi.org/10.1016/0300-9467(92)85004-S. URL http://www.sciencedirect.com/science/article/pii/030094679285004S.

R.H. Weiland, J. C. Dingman, and D. B. Cronin. Heat capacity of aqueous monoethanolamine, diethanolamine, n-methyldiethanolamine, and n-methyldiethanolamine-based blends with carbon dioxide. *Journal of Chemical & Engineering Data*, 42(5):1004–1006, 1997. doi: 10.1021/je960314v. URL http://dx.doi.org/10.1021/je960314v.

R. M. Wellek, R. J. Brunson, and F. H. Law. Enhancement factors for gas-absorption with second-order irreversible chemical reaction. *The Canadian Journal of Chemical Engineering*, 56(2):181–186, 1978. ISSN 1939-019X. doi: 10.1002/cjce.5450560205. URL http://dx.doi.org/10.1002/cjce.5450560205.

What'sYourImpact.org. Main sources of carbon dioxide emissions, 2016. URL http://whatsyourimpact.org/greenhouse-gases/carbon-dioxide-emissions.